Received: 29 April 2021 | Revised: 12 July 2021 | Accepted: 14 July 2021

DOI: 10.1002/wnan.1744

ADVANCED REVIEW

WIREs NANOMEDICINE AND NANOBIOTECHNOLOGY WILEY

Therapeutic gas delivery strategies

Wanjun Gong[1,2] | **Chao Xia**[2] | **Qianjun He**[2,3]

[1]Department of Pharmacy, Shenzhen Hospital, Southern Medical University, Shenzhen, China

[2]Guangdong Provincial Key Laboratory of Biomedical Measurements and Ultrasound Imaging, National-Regional Key Technology Engineering Laboratory for Medical Ultrasound, Marshall Laboratory of Biomedical Engineering, School of Biomedical Engineering, Health Science Center, Shenzhen University, Shenzhen, China

[3]Center of Hydrogen Science, Shanghai Jiao Tong University, Shanghai, China

Correspondence
Qianjun He, School of Biomedical Engineering, Health Science Center, Shenzhen University, Shenzhen, China.
Email: nanoflower@126.com

Funding information
Center of Hydrogen Science, Shanghai Jiao Tong University, China; National Natural Science Foundation of China, Grant/Award Number: 51872188; Special Funds for the Development of Strategic Emerging Industries in Shenzhen, Grant/Award Number: 20180309154519685; SZU Top Ranking Project, Grant/Award Number: 860-00000210

Edited by: Xiangyang Shi, Associate Editor and Gregory Lanza, Co-Editor-in-Chief

Abstract

Gas molecules with pharmaceutical effects offer emerging solutions to diseases. In addition to traditional medical gases including O_2 and NO, more gases such as H_2, H_2S, SO_2, and CO have recently been discovered to play important roles in various diseases. Though some issues need to be addressed before clinical application, the increasing attention to gas therapy clearly indicates the potentials of these gases for disease treatment. The most important and difficult part of developing gas therapy systems is to transport gas molecules of high diffusibility and penetrability to interesting targets. Given the particular importance of gas molecule delivery for gas therapy, distinguished strategies have been explored to improve gas delivery efficiency and controllable gas release. Here, we summarize the strategies of therapeutic gas delivery for gas therapy, including direct gas molecule delivery by chemical and physical absorption, inorganic/organic/hybrid gas prodrugs, and natural/artificial/hybrid catalyst delivery for gas generation. The advantages and shortcomings of these gas delivery strategies are analyzed. On this basis, intelligent gas delivery strategies and catalysts use in future gas therapy are discussed.

This article is categorized under:

Therapeutic Approaches and Drug Discovery > Emerging Technologies

Therapeutic Approaches and Drug Discovery > Nanomedicine for Oncologic Disease

KEYWORDS

gas delivery, gas therapy, nanomedicine

1 | INTRODUCTION

Initially, it was thought that gaseous NO (nitric oxide), CO (carbon monoxide), and H_2S (hydrogen sulfide) molecules were physiologically non-functional or even toxic to humans. Interestingly, when used at the appropriate concentration, these gases were found to be endogenous and necessary in the body, playing a very important role in a variety of biological processes (Chen et al., 2019; Wang, Yang, & He, 2020). With further researches, these gas molecules have been verified as messengers (named "gasotransmitters") in biological processes, which have a variety of physiological functions, including the regulation of the circulatory system, immune system, nervous system, and respiratory system (Vong & Nagasaki, 2020). One of the examples is NO, which was found to be a human endothelium-derived relaxation

factor in 1987 (Palmer et al., 1987). Mechanistically, these gasotransmitters mainly bind with hemoglobin to mediate signal transduction. For example, CO can regulate several important signaling pathways, including p38, MAPK, Erk1/2, JNK, Akt, NF-κB, and so on (Fujimoto et al., 2004; Ryter & Otterbein, 2004). CO/NO/H_2S, at a low concentration, have a protective effect on damaged cells by anti-inflammation but at a high concentration, exhibit obvious toxicity to cells, tissues, and blood owing to their inhibition to mitochondrial respiration (Motterlini & Otterbein, 2010; Wu & Wang, 2005). Therefore, targeted delivery of these toxic gases is vital.

Compared with NO, CO, and H_2S, hydrogen gas, which also has distinct anti-inflammatory effect, seems safer for humans. Dole et al. (1975) found that treatment of squamous carcinoma-carrying mice with 8 atm hydrogen gas can inhibit tumor growth effectively without visible toxic side effects. In 2007, Ohta reported that hydrogen can ameliorate cerebral ischemia–reperfusion injury by selectively reducing highly cytotoxic reactive oxygen species (ROS). Since then, hydrogen medicine has attracted worldwide attention (Ohsawa et al., 2007). The general routes of H_2 therapy include inhalation of hydrogen gas, oral intake of hydrogen-rich water (HRW), and injection of hydrogen-rich saline (HRS) (Y. Wu, Yuan, et al., 2019). The animal model revealed that, after intravenous injection of HRS, it takes 1 min for hydrogen concentration in the blood and tissues to reach the peak value, while, with oral intake of HRW, it takes 5 min (Liu et al., 2014). Due to excellent penetration property, hydrogen molecules can rapidly go through biological membranes, which also leads to the leakage of targeted delivery. It was found that inhalation of 3% hydrogen gas can make hydrogen molecules accumulate in the brain, liver, kidney, mesentery fat, and thigh muscle in a relatively low concentration (Yamamoto et al., 2019). Hence, how to accurately deliver these gas molecules to the lesion location is important to high efficacy of gas therapy.

As has been said, how to achieve targeted gas delivery and controlled release is the key issue in gas therapy. Naturally, various strategies for gas delivery have been developed. In this review, we focus on the recent significant progresses in the development of gas delivery strategies for gas therapy, and put gas delivery strategies into three categories: gas molecule delivery strategy, gas prodrug delivery strategy, and catalyst delivery strategy.

2 | GAS MOLECULE DELIVERY STRATEGY

In this section, we will introduce the strategy of directly delivering gas via adsorption approach (Table 1). This strategy involves the adsorption of therapeutic gas molecules into porous materials via two routes: (1) physical adsorption of gas molecules into porous nanocarriers (physisorption), and (2) chemical adsorption of gas molecules onto the interface with active anchoring sites (chemisorption).

2.1 | Physisorption

Physisorption, a general phenomenon, usually occurs when gas molecules are confined within adsorbents (Thommes, 2010). Due to the van der Waal attraction, multiple adsorption layers can be formed (Thommes & Cychosz, 2014). Microporous materials including metal–organic frameworks (MOFs) and zeolites are preferred for physical adsorption. The porous materials-based physisorption has been widely applied in gas adsorption, separation, and storage. However, emerging gas therapy sets down some specific requirements for gas storage and release.

Some MOFs including Ti-based MIP-177 (Figure 1a) and Zr-based UiO-66 (Figure 1b) were designed and developed for loading NO and O_2 gases by physisorption into their micropore channels (Gao et al., 2018; Pinto et al., 2020). Liposome and dendrimer were also the candidates for the gas carrier (Huang et al., 2009; Stasko & Schoenfisch, 2006). McPherson developed a liposome to carry NO gas molecules, having achieved a maximum NO loading capacity of 10 ml g^{-1} (Huang et al., 2009). The released NO can inhibit intimal hyperplasia in injured arterial segments, reducing thickened arterial wall by 41 ± 9%. Moreover, perfluorocarbon (PFC)-based microbubbles were broadly developed to carry oxygen and hydrogen gases based on good solubility of these gases in PFC (Figure 1c,d) (Cheng et al., 2015; He et al., 2017). The released O_2 can not only overcome the hypoxic microenvironment in the tumor but also improve the efficiency of photodynamic therapy and radiotherapy (RT) by enhancing tumor oxygenation. Ultrasound (US) imaging can be used to trace the microbubbles, and US stimulus can trigger the release of gas molecules in a controlled way. However, the H_2@PFC@Lip microbubble system is not stable as it can only remain effective for about 10 min.

TABLE 1 Gas molecule delivery strategy based on carrier-mediated physisorption and chemisorption

	Carrier	Delivery system	Advantage(s)	Delivered gas	References
Physisorption	MOFs	MIP-177	High storage capacity, no cytotoxicity, slow release	NO	Pinto et al. (2020)
		HKUST-1	Slow release		J. Chen, Sheng, et al. (2020)
		O_2@UiO-66@ICG@RBC	Long circulation and O_2 self-sufficient	O_2	Gao et al. (2018)
		UC@mSiO_2-RB@ZIFO_2-DOX-PEGFA	Upconversion nanoparticles for O_2-enhanced synergetic therapy		Xie et al. (2019)
	Liposome	NO-ELIP	Visualization delivery and controlled release	NO	Huang et al. (2009)
	Dendrimer	DAB-PO-64	High storage capacity	NO	Stasko and Schoenfisch (2006)
	Polymer	NG/DEN-F, NCNH/DEN-F	Slow release	NO	Krathumkhet et al. (2021)
	Hollow mesoporous organosilica NPs	IR780@O_2-FHMON	Ultrasonic stimulation release and ROS improvement	O_2	J. Chen, Luo, et al. (2017)
	Lipid microparticles	ICG@O_2-OI-MPs	Dual-mode theranostic agent for image-guided SDT with enhanced efficacy	O_2	Ma et al. (2017)
	PFC	O_2@PFC@Lip	Improved PDT efficacy	O_2	Cheng et al. (2015)
		PFC@O_2	Improved therapeutic outcomes in PDT and RT	O_2	X. Song, Feng, et al. (2016)
	Hollow Bi_2Se_3 NPs	PEG-Bi_2Se_3@PFC@O_2	Ability to overcome the hypoxia-associated radio-resistance of tumors	O_2	G. Song, Liang, et al. (2016)
	Microbubbles	H_2-MB	Image-guided hydrogen gas delivery	H_2	He et al. (2017)
Chemisorption	MOFs	$[M_2(C_8H_2O_6)(H_2O)_2]\cdot 8\ H_2O$ (M = Co, Ni)	High adsorption capacity, good storage stability, H_2O trigger	NO	McKinlay et al. (2008)
		MIL-88	Slow release		McKinlay et al. (2013)
		4-MAP modified HKUST-1	High storage capacity, no cytotoxicity, slow release		P. Zhang, Li, et al. (2020)
		UiO-66, UiO-66-NH_2, TIFSIX-2-Cu-i	Acid-trigger		Haikal et al. (2017)
		CPO-27	High storage capacity	H_2S	Allan et al. (2012)
		MIL-88B, MIL-88-NH_2	High storage capacity	CO	Ma et al. (2013)
		Cu doped ZIF-8	High storage capacity	O_2	Xie et al. (2019)
	Zeolite	ETS-4	High storage capacity	NO	Pinto et al. (2011)
		Cu-ETS-4	High storage capacity		Pinto et al. (2014)
		Al-EST-10 and Ga-EST-10	Low toxicity and slow NO release		Pinto et al. (2016)
		Zeolite-A	Relatively high capacity		Wheatley et al. (2006)
		Ze–NO	Absence of dramatic pro-inflammatory effects		Mowbray et al. (2008)
	HMSNs	HMSNs-LA-CO_2	US-trigger release bubbles in an on-demand manner	CO_2	K. Zhang, Xu, et al. (2015)

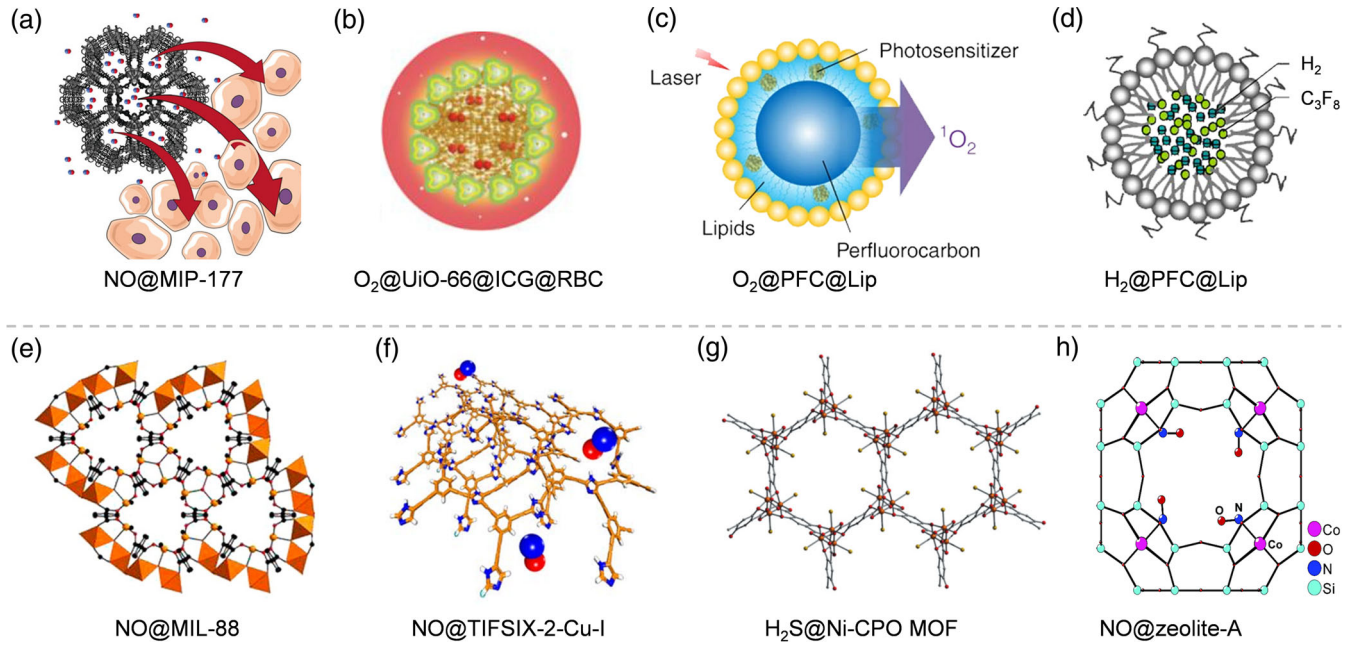

FIGURE 1 Typical examples of gaseous physisorption (a–d) and chemisorption (e–h) with various carriers. (a) NO gas delivery by MIP-177 (Pinto et al., 2020); (b) O_2 gas delivery by UiO-66@ICG@RBC (Gao et al., 2018); (c) O_2 gas delivery by PFC@Lip (Cheng et al., 2015); (d) H_2 gas delivery by PFC@Lip (He et al., 2017); (e) NO gas delivery by MIL-88 (McKinlay et al., 2013); (f) NO gas delivery by TIFSIX-2-Cu-I (Haikal et al., 2017); (g) H_2S gas delivery by CPO-27 (Allan et al., 2012); (h) NO gas delivery by zeolite-A (Wheatley et al., 2006)

2.2 | Chemisorption

Unlike physisorption, chemisorption is based on the chemical bond between host and guest molecules. It generally occurs only under specific conditions: for instance, inert gases have nothing to do with chemisorption. In addition, chemisorption cannot occur if the valence bond of surface atoms is already saturated with adjacent atoms. In chemisorption, the adsorption attraction is much stronger than the van der Waal force, and naturally the loading and controlled release of gases becomes easier than physisorption. What is more, the gaseous chemisorption capacity of carriers is mainly dependent on the amount and reactivity of surface-active sites rather than on the specific area and pore size of carriers alone.

Based on the coordination between transition metals (such as Co, Ni, Cu, Fe, Mn, etc.) with NO, CO, and H_2S, porous carriers with open active metal sites on the surface, typically zeolites and MOFs, are designed for chemisorption of these gases with therapeutic functions. As early as 2008, Morris et al. developed a kind of MOF (Co/Ni-MOF, $[M_2(C_8H_2O_6)(H_2O)_2]\cdot 8H_2O$ (M = Co, Ni)) for chemically adsorbing NO and H_2S gases into their pores (CPO-27-Co and CPO-27-Ni), showing high storage capacities of 7 and 6.2 mmol g^{-1} for NO and H_2S (Figure 1g), respectively (Allan et al., 2012; McKinlay et al., 2008). Due to the vasodilatory action of H_2S, H_2S released from CPO-27-Ni causes a significant substantial relaxation of the vessel after a short induction period (~5 min). In addition, the myography experiments revealed that NO-loaded CPO-27-Co can achieve controlled release of NO which causes the relaxation of porcine arterial tissue (Figure 1g) (Allan et al., 2012). Interestingly, the release performance is tunable by adjusting the coordination strength between metal ions and gas molecules. Similarly, Fe-based MIL-88, Cu-based ZIF-8, ETS-4, and LTA were also developed for chemically adsorbing NO, CO, and O_2 (Figure 1e,h) (Ma et al., 2013; McKinlay et al., 2013; Pinto et al., 2011; Pinto et al., 2014; Pinto et al., 2016; Wheatley et al., 2006; Xie et al., 2019).

In addition to coordination with metal ions, chemical bonding of gas molecules to organic groups on the surface of carriers can also be developed for gaseous chemisorption (Figure 1f) (Haikal et al., 2017). Xu et al. developed a 4-MAP (4-(methylamino) pyridine) modified HKUST-1 (named NMHK) to load NO gas by the route of chemisorption (P. Zhang, Li, et al., 2020). NO gas is bound to the secondary amino group via chemical bonds, which ensure a high NO storage capacity (4.8 times of unmodified HKUST-1). NO@NMHK showed a controlled and slow NO releasing performance with an average release rate of 1.67 nmol L^{-1} h^{-1} for more than 15 days. Although CO_2 has not shown significant therapeutic effects, it can be used to harmonize contrast-enhanced US imaging and to control the release of

therapeutic drugs. In light of the chemical reaction between CO_2 and primary or secondary amine groups, Shi prepared a L-arginine (LA)-modified hollow mesoporous silica nanoparticles (HMSNs) to capture and absorb CO_2. The chemical bond between CO_2 and amine group can be broken under US stimulation and acid environment, and thus the HMSNs-LA-CO_2 shows a dual-responsive release property (K. Zhang, Xu, et al., 2015).

3 | GAS PRODRUG DELIVERY STRATEGY

3.1 | Metal–CO/NO/H/S coordination compounds as gas prodrugs

Metal–CO/NO/H/H_2S coordination compounds are generally prepared by making use of the coordination between metal and carbonyl, nitrosyl, or hydrogen, and therefore can chemically decompose into CO, NO, H_2, or even H_2S (Xu et al., 2016) under excitation (Table 2). Such a coordination attraction is much stronger than physisorption/chemisorption, electrostatic interaction, and hydrogen bonding, and thus promises a kind of stable gas prodrugs. However, the bonds between metal and gas moiety are yet not as strong as covalent bonding, leading to easy responsive decomposition and release of gases upon a suitable stimulation, such as oxidation, heating, irradiation, and so on. In addition, the physicochemical properties of metal–CO/NO/H/H_2S coordination compounds, including stability and melting point, highly depend on the coordination attraction, and the solubility relies on the ligands linked to the metal center.

Good aqueous solubility of drugs is often desired for high bioaccessibility. Metal–CO/NO/H/H_2S coordination compounds without other ligands are highly hydrophobic, but modification with hydrophilic ligands can effectively improve their solubility. Some functional compounds involving glucose, vitamin B_{12}, and triphenylphosphine (TPP) can be conjugated onto these compounds for specific performances such as targeted delivery and high metabolism (Figure 2a) (Zobi et al., 2013). However, aqueous solubility-enhancing modification frequently causes the instability of the compounds. Quick spontaneous release of NO in physiological conditions is necessary for urgent therapy of myocardial ischemia diseases, while the sustained release of gases is required for long-term action, which can be tuned by decomposition reaction dynamics. On the other hand, aqueous insoluble gas prodrugs boast high stability, thus favorable for controlled gas release. In this case, some helpful carriers such as HMSNs and micelles can be used to load these insoluble prodrugs into their hydrophobic zone in order to improve their bioaccessibility.

Most metal–CO/NO coordination compounds, such as $Fe_3(CO)_{12}$, $Mn_2(CO)_{10}$, $Mn(CO)_5Br$, $Ru(CO)_5$, and $[Fe_4S_3(NO)_7](NH_4)_2$ (RBS), are sensitive to UV and visible light rather than near-infrared (NIR) light, limiting their bioapplications. The development of NIR-controlled gas release strategies based on metal–CO/NO coordination compounds is thus desired. Fortunately, the adsorption property of metal–CO/NO coordination compounds is tunable by replacing partial CO/NO with specific ligands (Chakraborty et al., 2014). Mascharak and coworkers coordinated $Mn(CO)_3Br$ with 2-phenylazopyridine, effectively shifting the adsorption band of $Mn(CO)_3Br$ towards infrared light and thus enabling NIR-responsive CO release (Figure 2b) (Carrington et al., 2013). Another route to NIR-sensitiveness is to conjugate metal–CO/NO coordination compounds to NIR-chromatic groups/ions/particles. Typically, co-precipitation of RBS^{2-} with NIR-adsorbing metal ions such as Cu^{2+} endows the formed insoluble Me-RBS with NIR adsorption and NIR-sensitive feature (Figure 2c) (L. Chen, He, et al., 2017). The conjugation of $Fe(NO)_2$ and $Mn(CO)_3Br$ onto porphyrin and graphene nanosheet enables the conversion of the NIR-light energy into chemical energy for photochemical degradation of gas prodrugs into NO and CO, respectively (Figure 2d) (He et al., 2015; Wecksler et al., 2006). Similarly, coordination and even incorporation of hydrogen into Pd nanoparticles or Pd-based MOF nanomaterials can also achieve NIR-responsive release of hydrogen gas owing to the NIR-adsorbing characteristics of these nanoparticles (Figure 2e,f) (Zhao et al., 2018; Zhou et al., 2019).

Moreover, the coordination interaction was found to be easily destroyed by oxidation with ROS for ROS-responsive gas release. We found that $Mn_2(CO)_{10}$ and $Fe_3(CO)_{12}$ can play a role as a Fenton-like agent to decompose intratumoral H_2O_2 into highly oxidative ·OH, which further oxidize these gas prodrugs to release CO gas, realizing intratumoral H_2O_2-responsive CO release and tumor-selective killing effect (Figure 2g) (Jin, Wen, Xiong, et al., 2017; Zhao et al., 2019). Based on this feature, iron carbonyl was conjugated with TPP^+ to realize mitochondria-targeted CO delivery and intramitochondrial controlled CO release, enhancing the efficacy of CO therapy of cancer (Figure 2h) (Meng et al., 2020). Like glutathione (GSH), Fe-CO can also release gas upon cysteamine (Cys) (Long et al., 2013) in the similar pathway.

TABLE 2 Gas prodrug delivery strategy

	Core structure	Delivery system	Trigger	Delivered gas	References
Metal-gas prodrugs	Pd-H	PdH-MOF	Spontaneous	H_2	Zhou et al. (2019)
	Mn-NO	$[Mn(PaPy_2Q)NO]ClO_4$	NIR light	NO	Eroy-Reveles et al. (2008)
		[Mn-NO]@MCM-41	Visible light	NO	Heilman et al. (2012)
	Mn-CO	PEG-BPY$[MnBr(CO)_3]$-GO	NIR light	CO	He et al. (2015)
		MCM@PEG-CO-DOX NPs	NIR light	CO	J. Yao, Liu, et al. (2019)
		HMOPM-CO	NIR light	CO	Tang et al. (2018)
		B12-MnCORM-1	NIR light	CO	Zobi et al. (2013)
		Ce6&CO@FADP	NIR light	CO	Ma et al. (2020)
		$[Mn(CO)_3(phen)(PTA)]CF_3SO_3$	Visible light	CO	Kawahara et al. (2017)
		CORMA-1-PLA	Visible light	CO	Bohlender et al. (2014)
		Ves-1.Mn	Visible light	CO	Sakla and Jose (2018)
		ALF472-cisplatin@Al-MCM41	Visible light	CO	Carmona et al. (2017)
		CORF-1	Visible light	CO	Diring et al. (2017)
		Ab-photoCORMs	Visible light	CO	Kawahara et al. (2020)
		PCL-Mn-PS	Visible light	CO	Askes et al. (2017)
		$[MnBr(azpy)(CO)_3]$	Visible light	CO	Carrington et al. (2013)
		MnCO@MPDA	H_2O_2 and H^+	CO	D. Wu, Duan, et al. (2019)
		MCMA NPs	H_2O_2 and H^+	CO	Y. Wang, Zhang, Lv, et al. (2020)
		UiO-type NMOF	H_2O_2 and H^+	CO	Guan et al. (2019)
		MnCO@hMSN	H_2O_2 and H^+	CO	Jin, Wen, Xiong, et al. (2017)
		MnCO@Ti-MOF	H_2O_2 and H^+	CO	Jin et al. (2018)
	Mn-S	MnS@BSA	H^+	H_2S	He et al. (2020)
	Ru-NO	N-GQDs@Ru-NO@Gal	NIR light	NO	Y. H. Li, Guo, et al. (2017)
	Ru-CO	CORM@IONP	Magnetic heating	CO	Kunz et al. (2013)
		Alginate@dextran@oximeCORM@IONP	Magnetic heating	CO	Meyer et al. (2016)
		Dextran500k@CORM@IONP	Heating	CO	Meyer et al. (2015)
		PA	Spontaneous	CO	Matson et al. (2012)
		CORM-3	Spontaneous	CO	Clark et al. (2003)
		COH	Spontaneous	CO	Kim et al. (2018)
		CONPs	Cys	CO	van der Vlies et al. (2016)
	Fe-NO	Me-RBS	NIR light	NO	L. Chen, He, et al. (2017)

TABLE 2 (Continued)

	Core structure	Delivery system	Trigger	Delivered gas	References
		PPIX-RSE	NIR light	NO	Wecksler et al. (2006)
		RBS-UCNPs	NIR light	NO	X. Zhang, Tian, et al. (2015)
		UPNCs@SiO_2	NIR light	NO	Garcia et al. (2012)
		RBS-T-UCNPs	NIR light	NO	X. Zhang, Guo, et al. (2017)
	Fe-CO	$[Fe_2(\mu\text{-}SCH_2CH(OH)CH_2(OH))_2(CO)_6]$	Cys	CO	Long et al. (2013)
		FeCO-MnO_2@MSN	ROS	CO	Zhao et al. (2019)
		FeCO-TPP@MSN@HA	ROS	CO	Meng et al. (2020)
		m-PB-CO/PEG NPs	NIR light	CO	Li et al. (2016)
		eCO-DOX@MCN	NIR light	CO	X. Yao, Yang, et al. (2019)
		PPPPB–CO NPs	NIR light	CO	Boakye-Yiadom et al. (2019)
		ET-CORMs	Penicillin gamidase	CO	Meng et al. (2020)
		(Re-CO)@Al-MCM-41	Visible light	CO	Chakraborty et al. (2015)
		ReCMCS	Visible light	CO	Chakraborty et al. (2017)
	Fe-S	FeS@BSA	Acid	H_2S	Xie et al. (2020)
	Mo	TTM	Acid	H_2S	Xu et al. (2016)
Redox based prodrugs		GSNO-loaded $CaCO_3$	GSH/Cu^+	NO	Lee et al. (2016)
		GCZ@M	US	NO	An et al. (2020)
		GSNO/$Cu_{1.6}S$-PLGA	GSH/Cu^+	NO	Kao et al. (2017)
	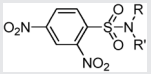	2,4-Dinitrophenylsulfonamides	RSH	SO_2	Malwal et al. (2012)
		BODS NPs	pH/GSH	SO_2	Gu et al. (2020)
		mPEG-PLG (DNs)	GSH	SO_2	Y. Zhang, Shen, et al. (2020)
	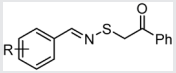	SATO-micelle	GSH	H_2S	Foster et al. (2017)
	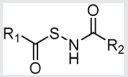	*N*-(Acylthio)amides	GSH	H_2S	Zhao et al. (2015)
		Arylthioamides	GSH	H_2S	Martelli et al. (2013)
	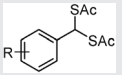	TAGDD-1	GSH	H_2S	Zhao et al. (2014)
	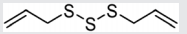	DATS-MSN	GSH	H_2S	Sun et al. (2015)
		AB-DS@BSA-N_3 NYs	GSH	H_2S	Zheng et al. (2020)

(Continues)

TABLE 2 (Continued)

	Core structure	Delivery system	Trigger	Delivered gas	References
	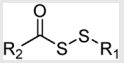	Perthiol	GSH/Cys	H_2S	Zhao et al. (2013)
	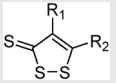	H_2S-DOXOs	GSH	H_2S	Chegaev et al. (2016)
		PEG–ADT	GSH		Hasegawa and van der Vlies (2014)
Hydrolysable gas prodrugs		Hollow microsphere	Acid	H_2S	Chung et al. (2015)
	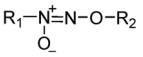	meGal-No A4-β-gal	Enzymes	NO	Hou et al. (2019)
		IPA/NO and DEA/NO	Acid		Basudhar et al. (2013)
		PINM	NIR light		An et al. (2020)
		CaP-NONO	Acid		Choi et al. (2016)
	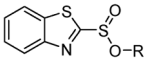	BTS	Spontaneous	SO_2	Day et al. (2016)
		GNRs@PDA-BTS	Acid and light		Lu et al. (2020)
		Au–Ag-BTS HTNs	Acid		Xu et al. (2020)
	Carbonate	Bubble-generating nanosystem	Acid	CO_2	Yang et al. (2016)
		DOX-$CaCO_3$-MNPs	Acid		Min et al. (2015)
		mCNP-DOX	Acid		Jang et al. (2018)
		HMME/MCC-HA	Acid and US		Feng et al. (2018)
	Mg	Mg@PLGA MPs	Spontaneous	H_2	Wan et al. (2018)
		Mg@p-SiO_2 MPs	Spontaneous	H_2	Kong et al. (2019)
	NH_3BH_3	AB@MSN	Acid	H_2	Yang et al. (2018)
		mPDAB	Acid	H_2	C. Zhang, Zheng, et al. (2019)
		AB@hMSN	Acid	H_2	Wang et al. (2021)
	MgB_2	MBN@PVP	Acid	H_2	Fan et al. (2019)
	Fe	Fe@CMC	Acid	H_2	Kou et al. (2019)
Diels–Alder reaction-based gas prodrugs	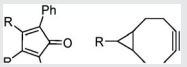	TPCPD and exo-BCN	Spontaneous	CO	D. Wang, Viennois, et al. (2014)
		TPP-dienone	Concentration	CO	Y. Zheng, Ji, et al. (2018)
	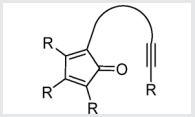	BW-CP-101-107	Spontaneous	CO	Ji et al. (2016)
		BW-ETCO-101/102	Esterase	CO	Ji, Ji, et al. (2017)

TABLE 2 (Continued)

	Core structure	Delivery system	Trigger	Delivered gas	References
		BW-CO-201–205	pH	CO	Ji, De La Cruz, et al. (2017)
	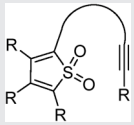	S-dioxide	Spontaneous	SO_2	Ji, El-Labbad, et al. (2017), Wang et al. (2017)
Photo/sound/X-ray responsive prodrugs		Nitroimidazole	Visible light	NO	Diring et al. (2013)
	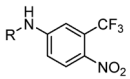	DPP-NF NPs	Visible light	NO	Y. Wang, Huang, et al. (2018)
	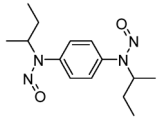	mPEG-PLGA-BNN6-DOX	UV/Vis light	NO	Fan et al. (2016)
		GO–BNN6	NIR light	NO	J. Fan, He, et al. (2015)
		BNN-Bi_2S_3	NIR light	NO	X. Zhang, Du, et al. (2019)
		BNN6-SPION@hMSN	US	NO	Jin, Wen, Hu, et al. (2017)
	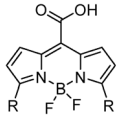	COR-BDPs	NIR	CO	Palao et al. (2016)
	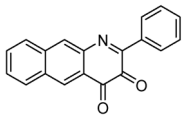	Flavonol–borate	H_2O_2	CO	Popova et al. (2018)
	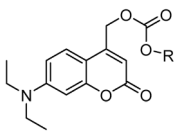	DEACM-PEG	Light	CO_2	Y. Zhang, Guan, et al. (2017)
	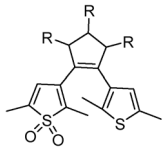	Diarylethene	UV light	SO_2	Kodama et al. (2015), Li et al. (2019)
	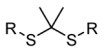	SP	Thiol	H_2S	W. Chen, Chen, et al. (2015)

(Continues)

TABLE 2 (Continued)

Core structure	Delivery system	Trigger	Delivered gas	References
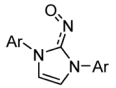	(IPrNO) IMesNO	Heating	NO	Park et al. (2015)
	IMesNO@MCs	HIFU	NO	Kang et al. (2019)
	CuS-PEI/NO-TPP	NIR light	NO	Wu et al. (2020)
S-NO	PTNGs	NIR	NO	Guo et al. (2017)
	PEG-USMSs-SNO	X-ray	NO	W. Fan, Bu, et al. (2015)
NH_4HCO_3	NH_4HCO_3 liposomes	Heating	CO_2	Chung et al. (2012)
	CO_2-generating liposomal	Heating	CO_2	Han et al. (2015)
	CO_2-generating liposomal	NIR light	CO_2	Chuang et al. (2016)

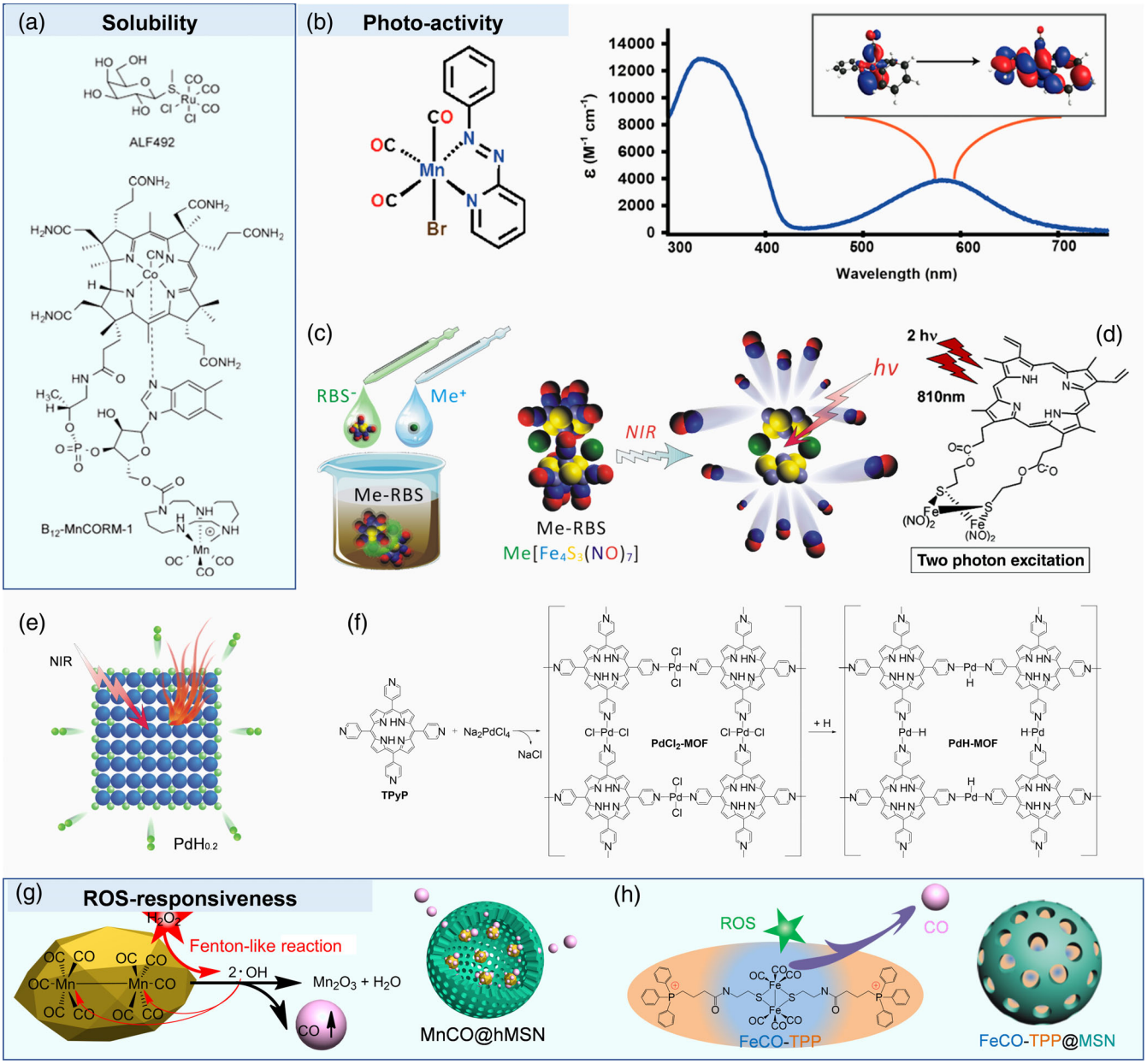

FIGURE 2 Gas delivered by metal-gas prodrugs. (a) Water soluble metal-gas prodrug for CO delivery based on B_{12}-MnCORM-1 (Zobi et al., 2013); (b) legends induced red shifting in absorbance (Carrington et al., 2013); (c) NIR responsive Me-RBS for NO delivery (L. Chen, He, et al., 2017); (d) NIR responsive PPIX-RSE for NO delivery (Wecksler et al., 2006); (e) NIR responsive $PdH_{0.2}$ for H_2 delivery (Zhao et al., 2018); (f) NIR responsive Pd-MOF for H_2 delivery (Zhou et al., 2019); (g) ROS responsive MnCO@hMSN for CO delivery (Jin, Wen, Xiong, et al., 2017); (h) ROS responsive FeCO-TPP@MSN@HA for CO delivery (Meng et al., 2020)

3.2 | Redox-induced gas-generating prodrugs

Specific microenvironments in the diseased site such as reductive and acidic conditions in the tumor microenvironment (TME) can be developed as physiological stimuli trigger for drug release. GSH concentration in tumor cells is approximately 5000-fold higher than that in normal cells (Tew et al., 2011). Thus, a large number of redox-induced gas-generating prodrugs have been designed, the commonest of which contains thiol groups, including diallyl sulfide (DAS), diallyl disulfide (DADS), diallyl trisulfide (DATS), S-allylcysteine, dithiothreitol, arylthioamide, N-mercapto-based H_2S donor, and their derivatives. DAS, DADS, and DATS are naturally existent molecules which can produce H_2S in certain conditions, but their naked structure is not suitable for long-time delivery and precise targeting. Thus, based on the structure of those compounds, several kinds of H_2S prodrugs were designed to involve N—SH, S—S

(Zhao et al., 2013), S—S—S (Roger et al., 2013; Sun et al., 2015; Zhao et al., 2014), and cyclic S—S═S bonds (Chegaev et al., 2016; Hasegawa & van der Vlies, 2014). Typically, by an exchange reaction, high concentrations of GSH and Cys can break the N—SH and S—S links to respectively form H_2S and RSSH, which further reacts with GSH to generate H_2S (Figure 3a) (Citi et al., 2014; Martelli et al., 2013; Martelli et al., 2014). The release rate of H_2S can be well adjusted by controlling the concentrations of GSH and Cys and the exchange reaction dynamics.

RSH mediated thiol attacks the carbon adjacent to the sulfur on 2,4-dinitrophenylsulfonamides and causes proton transfer from thiol to amide, leading to decomposition of sulfonamides and release of SO_2 (Figure 3b) (Malwal et al., 2012). The rate constant of SO_2 generation (k) depends on the stability of the transition state leading to the formation of protonated amine intermediate II, and thus stronger basicity (or weaker conjugate acid) will result in higher k. This strategy was adopted to build SO_2 prodrugs for gas therapy of cancer (Gu et al., 2020; Y. Zhang, Shen, et al., 2020), and the SO_2 released from those prodrugs was found to increase ROS level, mainly O_2^{-}, and show a remarkable tumor suppression efficacy. On the other hand, the breakdown of S—NO bond can also produce NO by a redox reaction. Besides GSH, other reductive agents such as Cu^{+} derived from nanocarriers can also be used to trigger the redox reaction for NO generation (Figure 3c) (Kao et al., 2017).

3.3 | Diels–Alder (click) reaction-based gas prodrugs

Bioorthogonal chemistry was widely used for biomarking in the living system. Just like the highly efficient cycloaddition between cyclooctyne and azide, the reaction between cyclooctyne and alkene can also form a cyclo-compound, when the generated dienone decomposes to release CO by the D–A (click) reaction. But the regular D–A reaction involving dienone always requires a high temperature and thus has difficulty in releasing CO in vivo. To address this issue, Wang chose bicyclo-[6.1.0]nonyne (BCN) as cyclooctyne and tetraphenylcyclopentadienone (TPCPD) as CO donor for the D–A reaction (D. Wang, Viennois, et al., 2014). On one hand, the high strain force of BCN increases the energy gap, which makes the D–A reaction easier to occur. On the other hand, the carbonyl group in TPCPD can be released as CO upon the D–A reaction. Combination of the two compounds will make a click-and-release approach to CO delivery. Later, they replace the activated alkyne with the acyclopentadienone-tethering one to achieve an intramolecular cycloaddition reaction (Figure 4a) (Ji et al., 2016), but it is very hard to balance the stability and controlled CO release (Pan et al., 2017). In order to achieve the on-demand release of CO, an esterase-activated method was designed based on the intramolecular D–A reaction (Ji, Ji, et al., 2017). Besides the esterase-activated CO release, the pH-triggered and concentration-dependent CO release for tumor-targeted delivery was also developed (Ji, De La Cruz, et al., 2017; Y. Zheng, Ji, et al., 2018).

In addition to CO delivery, this click reaction-based approach can also be adopted for SO_2 and H_2S delivery. For example, the replacement of the carbonyl group of prodrugs by O═S═O can achieve controlled SO_2 release by a similar D–A reaction (Figure 4b) (Ji, El-Labbad, et al., 2017; Wang et al., 2017). The case of H_2S is a bit different, such as the

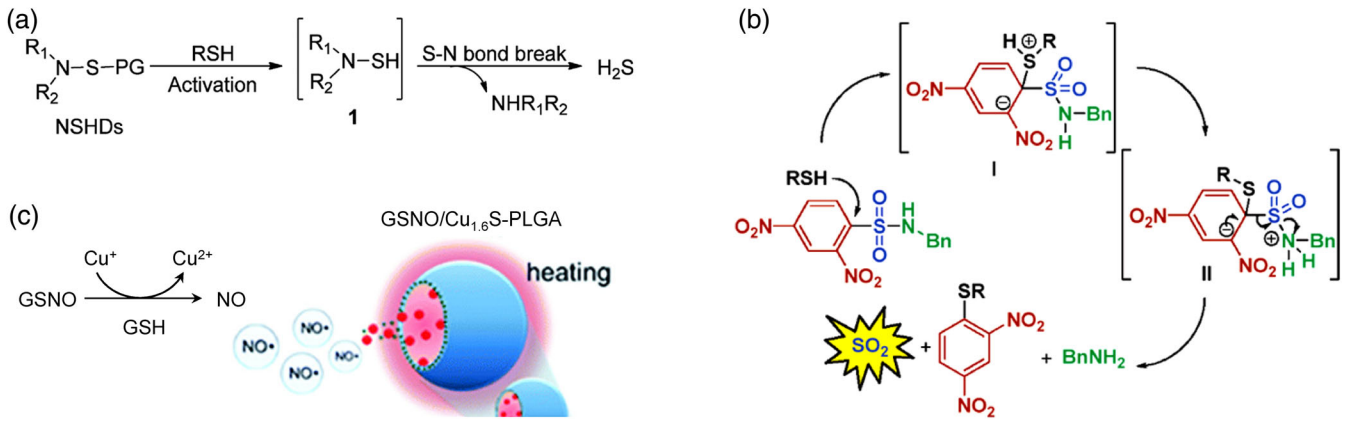

FIGURE 3 Typical redox-based gas prodrugs for gas delivery. (a) RSH triggered H_2S delivery (Citi et al., 2014; Martelli et al., 2013; Martelli et al., 2014); (b) RSH triggered SO_2 delivery (Malwal et al., 2012); (c) GSH triggered NO delivery (Kao et al., 2017)

pairs of trans-cyclooctene and tetrazine or mesoionic compound and strained alkyne (Figure 4c) (Steiger et al., 2017), but this strategy has not been applied in H_2S gas therapy so far.

3.4 | Hydrolysable gas prodrugs

Hydrolysis refers to the reaction between a chemical compound and water, and the acidic microenvironment of many diseases such as solid tumors usually can accelerate the reaction for gas release from some acid-sensitive gas prodrugs such as NONOates (Basudhar et al., 2013), BTS (Day et al., 2016; Lu et al., 2020), carbonic acid salt (Yang et al., 2016), and ammonia borane (Yang et al., 2018). Some nanocarriers including MSNs can be used to encapsulate and stabilize them for controlled gas release (Choi et al., 2016; Feng et al., 2018; Jang et al., 2018; Kong et al., 2019; Min et al., 2015; Wan et al., 2018; C. Zhang, Zheng, et al., 2019). For gas prodrugs with low reactivity with water such as Fe and metal borides (Fan et al., 2019; Kou et al., 2019), nano-sizing can effectively enhance their reactivity, enabling the acid-responsive hydrolysis-driving release of hydrogen gas. In an example, Zhao protected NONOates from hydrolysis by caging them within galactose (Wu et al., 2001). By the recognition between the designed unique galactose and the corresponding specific enzyme, a "bump-and-hole" delivery system was designed to achieve precise NO delivery, effectively reducing side effects and markedly enhancing NO therapeutic efficacy in the treatment of ischemic diseases (Hou et al., 2019).

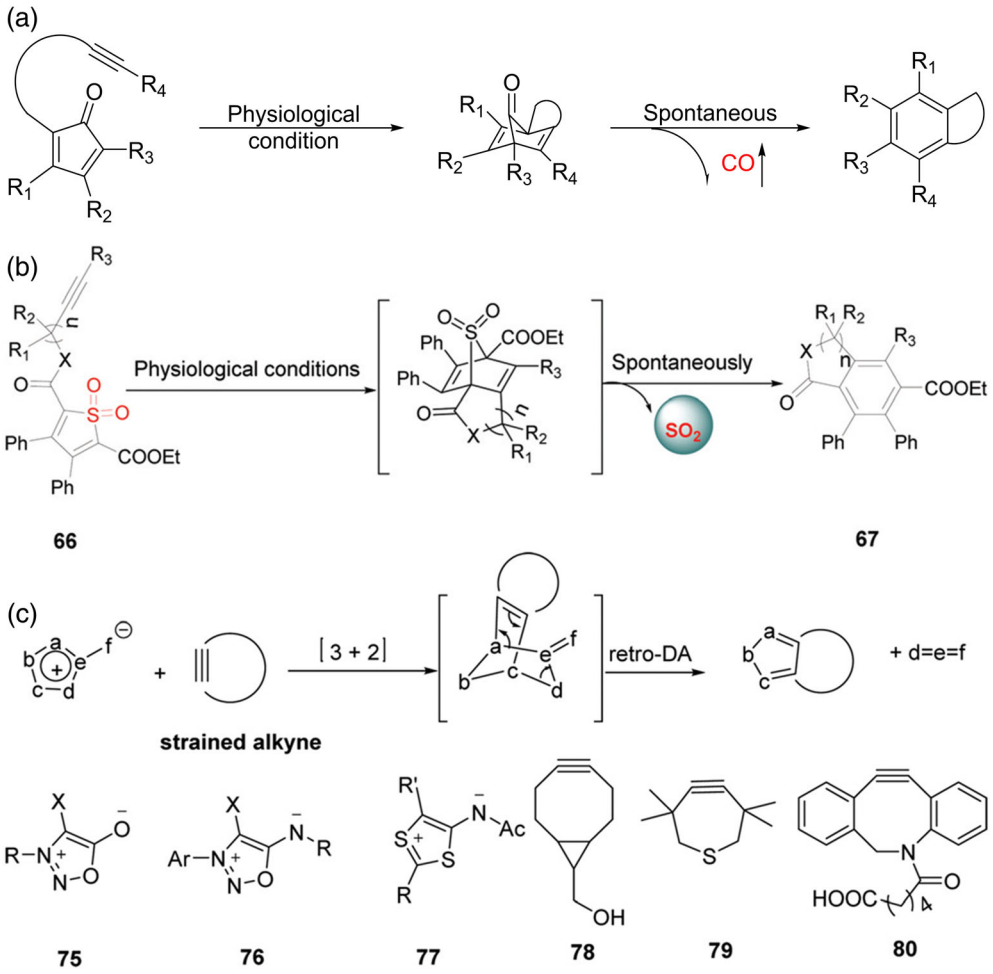

FIGURE 4 Typical click reaction-based prodrugs for gas delivery. (a) Unimolecular prodrug for CO delivery (Ji et al., 2016); (b) unimolecular prodrug for SO_2 delivery (Ji, El-Labbad, et al., 2017; Wang et al., 2017); (c) click reaction based H_2S delivery (Steiger et al., 2017)

3.5 | Photo/sound/X-ray-responsive gas prodrugs

The discovery and development of external stimuli-sensitive gas prodrugs are of significance as external stimuli sources can be easily operated and controlled. Many gas prodrugs have been found to be sensitive to UV and visible light, such as metal–CO/NO coordination compounds (Figure 2). Their sensitive adsorption bands can be shifted to the NIR zone by coordinating with specific ligands or by conjugation with NIR-chromatic groups/ions/particles (such as GON, BPN, and UCNP). As for those small organic molecules which are stable under irradiation, they can be modified to make photosensitive gas prodrugs. Klán modified the meso position of BODIPY with a carboxylic acid to develop a UV/Vis/NIR-responsive CO prodrug (COR-BDP, Figure 5a) (Palao et al., 2016). Under light irradiation, COR-BDP follows the usual pathway from excited singlet state to triplet state via intersystem crossing, and the formed diradical is not stable and thus quickly turns to α-lactone, which decomposes to generate CO (Figure 5b). Moreover, CO release from COR-BDP is accompanied by an obvious change in fluorescence intensity, and thus the CO release process can be facilely monitored in vivo without the need for any external marker.

NIR laser is relatively inexpensive and facilely operable, but its tissue penetration capability is still limited (<1 cm). By comparison, US has higher tissue penetration capability (20 cm), and its frequency, power, and focus can all be controlled. It was found that BNN is responsive to both UV light and US. US can boost the generation of free radical NO and thus facilitate the decomposition of BNN to release NO (Figure 5c,d) (Jin, Wen, Hu, et al., 2017). Fe_3O_4 nanoparticle-encapsulated hMSN was once used to load hydrophobic BNN in a high capacity for tumor-targeted delivery and MRI-guided controlled NO release (Ji, De La Cruz, et al., 2017). And, the SNO-type NO prodrug was found to promote NO release under X-ray and therefore can be used to sensitize RT (W. Fan, Bu, et al., 2015). X-ray and magnetic fields have higher tissue penetration capability, but gas prodrugs sensitive to these stimuli are rarely explored and thus are worthy of serious attention.

4 | GAS GENERATION-ENABLED CATALYST DELIVERY STRATEGY

Besides delivering gas molecules and their prodrugs, local generation of therapeutic gas molecules through catalytic reactions can also supply gas for therapy. This strategy needs catalyst delivery, substrate (sacrifice agent) supply, and appropriate excitation with external energy sources such as light, sound, or magnet. According to the type of catalysts,

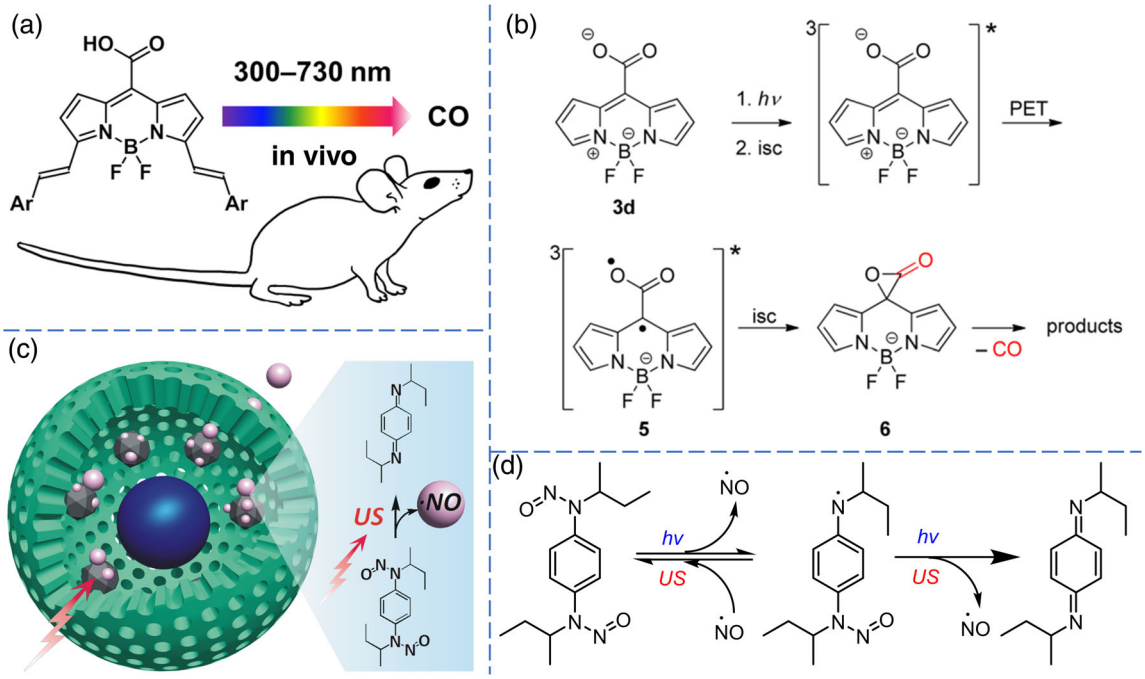

FIGURE 5 Typical photo/sound responsive gas prodrugs for gas delivery. (a,b) Photo-triggered CO release based on BODIPY and its mechanism (Palao et al., 2016); (c,d) US-triggered NO release based on BNN and its mechanism (Jin, Wen, Hu, et al., 2017)

this section will introduce three typical catalyst delivery strategies: semiconductor delivery, enzyme delivery, and hybrid catalyst delivery (Table 3).

4.1 | Semiconductor delivery

Semiconductor materials are the most common catalysts and have been widely used for organics degradation, water splitting, and air purification successfully (S. Chen, Takata, & Domen, 2017; Mamaghani et al., 2017; C.-C. Wang, Li, et al., 2014). Inspired by the photosynthesis of plants, Sung et al. designed and constructed a AA-AuNPs-chlα@Lip nanomedicine by encapsulating chlorophyll α (chlα), AA (L-ascorbic acid), and Au nanoparticles (AuNPs) into Lip (liposome) (Wan et al., 2017). Under the illumination of 660 nm laser, chlα is excited (chlα*) to produce electron–hole pairs, and then AuNPs collect electrons from chlα* to generate H_2 gas when holes oxidize the substrate AA. However, the tissue penetration depth of 660 nm laser is not desirable and the substrate loading capacity of the nanomedicine limits the amount of hydrogen generated. To resolve this, Sung further developed a CIT-UCNP-AuNPs-Chlα@Lip nanomedicine to realize NIR-responsive hydrogen generation by using UCNP to convert NIR light to UV/Vis light for photocatalysis (Figure 6b) (Wan et al., 2020). Locally generated H_2 can eliminate inflammation and restore ROS homeostasis by scavenging excessive ROS. Although in both cases hydrogen can be produced locally in the lesion through the photocatalytic approach, the hydrogen production is not efficient due to the need of co-delivering exogenous substances (AA and CIT) as sacrifice agents. Recently, we reported a H_2 supply method through direct NIR-photocatalysis which was realized by a Z-scheme $SnS_{1.68}$-$WO_{2.41}$ nano-catalyst developed, and a suitable band structure enabled hydrogen generation and hole-mediated oxidation of intratumoral over-expressed GSH under the illumination of 808 nm laser, realizing the combination of hydrogen/hole therapies for efficient modulation of the TME (Figure 6d) (Zhao et al., 2021). It is especially worth mentioning that no need for carrying sacrifice agents enables sustainable and repeatable hydrogen generation for long-term cancer therapy.

Zhang et al. developed an innovative nano-catalyst, which was constructed by co-loading histidine-rich peptide (CHHHHGRGD) and Ag_3PO_4 nanoparticles onto the carbon-dot-decorated C_3N_4 nanoparticle (HisAgCCN), to achieve visible-photocatalytic reduction of endogenous CO_2 into CO (Figure 6c) (Zheng et al., 2017). Furthermore, they developed WO_3 nanosheets to realize NIR-photocatalytic CO generation from CO_2 (S.-B. Wang, Zhang, Ye, et al., 2020). In addition, *E. coli* (*Escherichia coli*) was used to load carbon-dot-decorated C_3N_4 (CCN@*E. coli*) to achieve a photocatalytic reduction of endogenous NO_3^- into NO for tumor-targeted therapy (Figure 6a) (D.-W. Zheng, Chen, et al., 2018). Recently, Yang et al. developed an X-ray triggering sustainable H_2 producing platform (Au–TiO_2@ZnS), composed of Au–amorphous TiO_2 nano-dumbbell-shaped heterostructure coated with long afterglow ZnS particles, for synergistic H_2-RT of cancer. Since X-ray has remarkably higher tissue penetration capability compared with light and sound, the X-ray-catalytic gas delivery strategy is of high significance to gaseous sensitization of RT (Wu et al., 2021).

4.2 | Enzyme delivery

Enzymes, which are a kind of natural protein catalysts, wildly exist in the body and playing various important physiological roles. Compared with semiconductor catalysts, enzymes can catalyze special chemical reactions under physiological conditions with high catalytic efficacy (Yang et al., 2019). However, enzymes are generally not so stable, which can be resolved by protection with nanocarriers. Many enzymes can be utilized for gas therapy. This section will introduce the enzyme delivery strategy for gas therapy.

In order to address the long-term oxygen demand for diabetic foot treatment, H. Chen, Cheng, et al. (2020) developed a patch dressing (AGP) by loading photosensitive oxygen-generating living microalgae into calcium alginate gel (Figure 7a). Compared with topical gaseous oxygen therapy, AGP can release oxygen gas locally on demand by adjusting the switch and intensity of light resources, showing obvious advantages in deep oxygen delivery. Stevens et al. developed a poly(methacrylic acid) capsule and a 1-palmitoyl-2-oleoyl-sn-glycero-3-phosphocholine (POPC) liposome to encapsulate β-galactosidase (enzyme) and galactose-caged NONOate (β-gal-NONOate, NO prodrug/substrate), respectively, for the development of two nanomedicines (Chandrawati et al., 2017). After directly targeting the conventional outflow pathway, the degradation of POPC liposome causes a slow release of β-gal-NONOate which consequently decomposes into NO under the catalysis of β-galactosidase (Figure 7b).

TABLE 3 Catalyst delivery strategy for catalytic gas generation

	Delivery system	Advantage(s)	Delivered gas	References
Semiconductor catalysts	Chlα-AA-Au@liposome	Locally providing a high therapeutic concentration	H_2	Wan et al. (2017)
	CIT-UCNP-AuNPs-Chlα@Lip	Bio-imaging and therapy in situ	H_2	Wan et al. (2020)
	$SnS_{1.68}$-$WO_{2.41}$	Endogenous sacrifice agent, combined hole/hydrogen therapy	H_2	Zhao et al. (2021)
	Pdot-AA@ liposome	In situ hydrogen therapy	H_2	B. Zhang, Wang, et al. (2019)
	UCNPs/g-C_3N_4/Cu_3P	H_2-mediated cascade-amplifying multimodal synergetic therapy	H_2	Q. Wang, Ji, Shi, and Wang (2020)
	Au–TiO_2@ZnS	Synergistic H_2-radiotherapy Higher tissue penetration capability	H_2	Wu et al. (2021)
	Fe-C_3N_4@Ru@HOP	Enhanced antitumor efficacy of PDT	O_2	Y. Zhang, Bo, et al. (2019)
	C-dot/Ag_3PO4-C_3N_4-RGO	Aggravating oxidative stress ability	CO	Zheng et al. (2017)
	Pt-CuS Janus	Photothermal enhancement of the catalytic activity	CO	Liang et al. (2019)
	PEG@DW/BC	Anti-inflammatory	CO	S.-B. Wang, Zhang, Ye, et al. (2020)
Enzyme catalysts	CCN@*E. coli*	Photo-controlled bacterial metabolite therapy	NO	D.-W. Zheng, Chen, et al. (2018)
	3MST	—	H_2S	Mikami et al. (2011)
	QM-NPQ@PDHNs	GSH trigger release, low-toxic	NO	Jia et al. (2018)
	β-gal-NONOate	Localized therapeutic delivery with intraocular pressure reduced	NO	Chandrawati et al. (2017)
	iNOs	Good biocompatibility	CO	Romanski et al. (2012)
	pig liver esterase and lipas	Good biocompatibility	CO	Botov et al. (2013)
	AGP	Excellent skin permeability	O_2	H. Chen, Cheng, et al. (2020)
	PLGA NPs	Selectively unload, ability to overcome multi-drug resistance	O_2	Chen et al. (2014)
	catalase@MONs	Long-term cancer starvation therapy and robust PDT	O_2	Liu et al. (2017)
	HAOP NP	H_2O_2-triggered PDT	O_2	H. Chen, Tian, et al. (2015)
	IONPs	Relieving tumor hypoxia, photothermal imaging, for precisely guiding cancer therapy	O_2	Chen et al. (2012)
	MnO_2@PtCo	Relieving hypoxia, inducing cell apoptosis	O_2	Z. Wang, Zhang, et al. (2018)
	MnO_2	Improved intratumoral diffusion and TME modulation	O_2	Chen et al. (2016)
	mCGP	Starving /PDT therapy	O_2	S.-Y. Li, Cheng, et al. (2017)
Hybrid catalysts	ceCyan	Enhanced PDT	O_2	Huo et al. (2020)
	S-UCNP-Ce6 complex	Enhanced PDT	O_2	Zhang et al. (2021)
	[FeFe]TPP/GEM/FCS	Multidrug-resistance reversal	H_2	Sun et al. (2020)

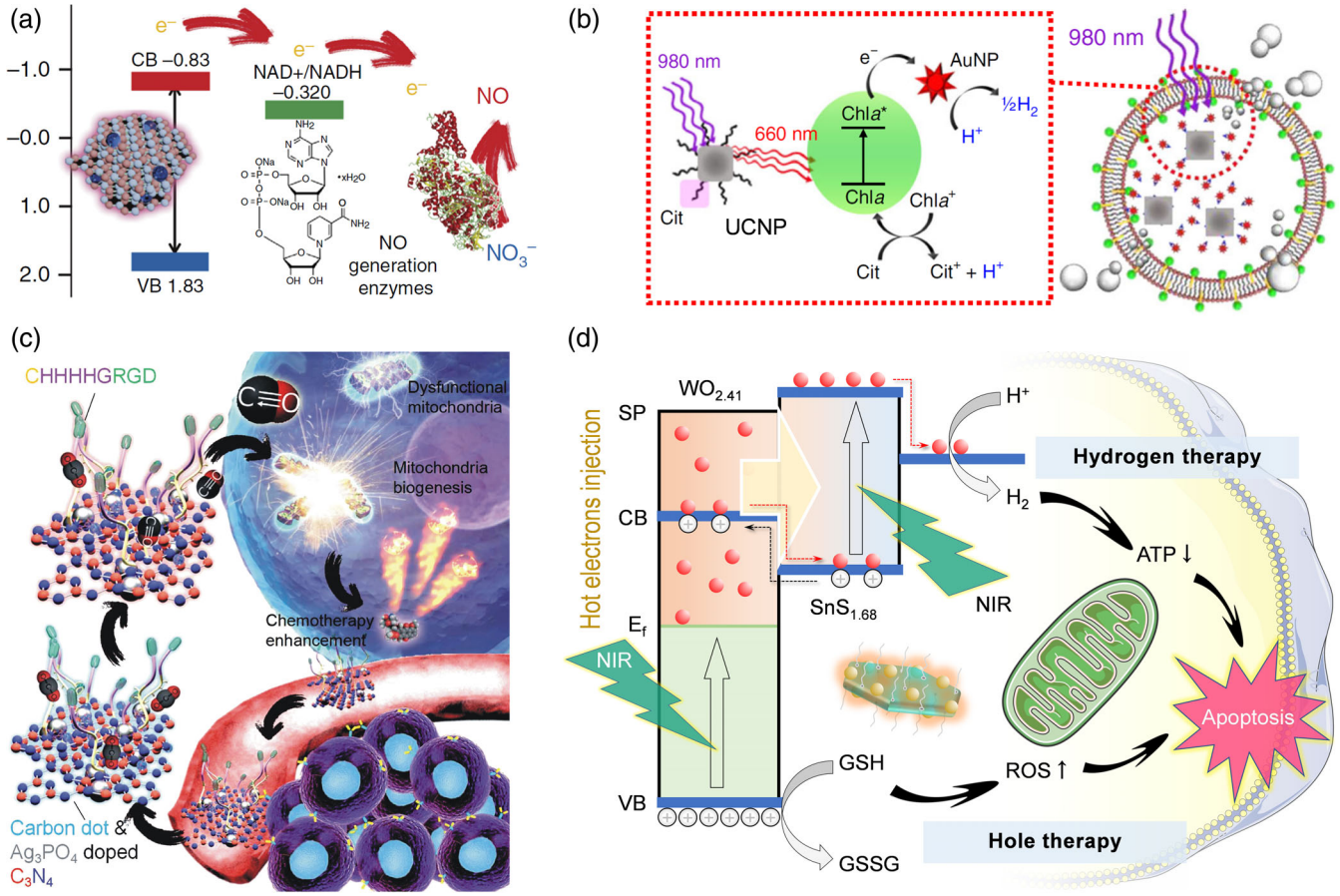

FIGURE 6 Photocatalytic strategy for gas delivery. (a) NO gas delivery by CCN@*E. coli* (D.-W. Zheng, Chen, et al., 2018); (b) H_2 gas delivery by CIT-UCNP-AuNPs-Chlα@Lip (Wan et al., 2020); (c) CO gas delivery by HisAgCCN (Zheng et al., 2017); (d) H_2 gas delivery by $SnS_{1.68}$-$WO_{2.41}$ (Zhao et al., 2021)

3-Mercaptopyruvate sulfurtransferase (3MST) can catalyze 3-mercaptopyruvate to produce H_2S (Mikami et al., 2011). The activity of 3MST is regulated by redox change and 3MST makes a certain contribution to maintaining redox homeostasis and serves as an antioxidative protein. This feature might favor microenvironment responsive gas generation by 3MST enzyme delivery. On the other hand, based on specific enzyme over-expression in the microenvironment of diseases, corresponding substrates for gas generation can be delivered for gas therapy (Jia et al., 2018).

In addition to natural enzymes, artificial nanoenzymes can also play the role of producing gas for disease treatment (Chen et al., 2012). Qu et al. designed and developed MnO_2@PtCo nanoflowers, where PtCo and MnO_2 functioned as oxidase and catalase mimic, respectively (Z. Wang, Zhang, et al., 2018). The MnO_2@PtCo nanoflowers can not only alleviate the hypoxia state in tumors but also significantly induce cancer apoptosis through ROS-mediation, leading to significant inhibition of tumor growth.

4.3 | Hybrid catalyst delivery

Enzymes have a powerful function in physiological conditions but have limitations in physicochemical functions for the generation of therapeutic gases. Artificial semiconductor catalysts possess tunable physicochemical functions but cannot completely mimic the catalytic roles of natural enzymes. Therefore, in order to combine the advantages of enzymes and semiconductors, hybrid catalysts were developed for efficient gas production.

Recently, photocatalytic synthesis systems based on enzymes and semiconductors have been designed and fabricated for efficient solar conversion successfully. Although this kind of hybrid catalyst system has not been used for gas therapy, it is worthy of attention. Zhong et al. constructed a semi-artificial photosynthesis system via anchoring $Cd_{0.9}Se_{0.1}S$/CdSeS@ZnS QDs (quantum dots) on the curli fibers in the biofilm (Wang et al., 2019). Meanwhile, they

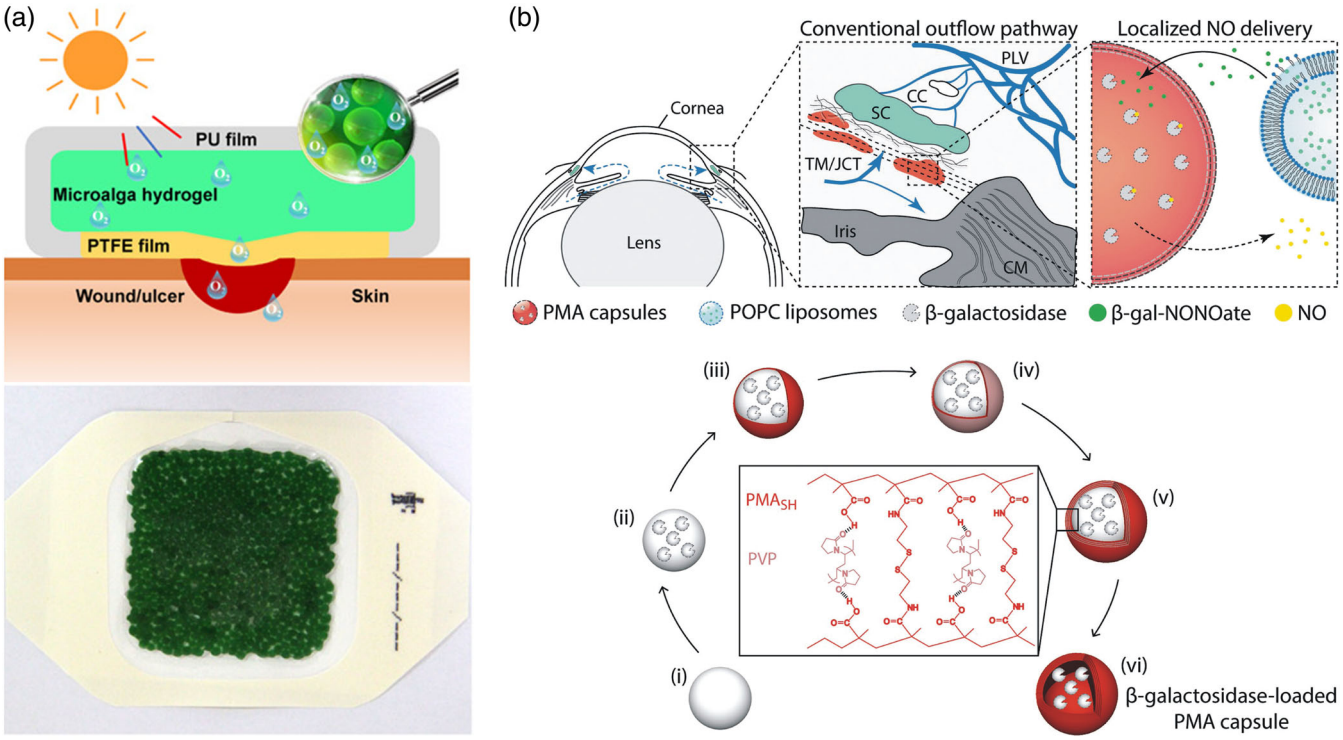

FIGURE 7 Enzyme delivery for gas generation. (a) The microalga-encapsulated photocatalytic oxygen-generating patch for wound healing (H. Chen, Cheng, et al., 2020); (b) localized delivery of NO to the conventional outflow pathway (Chandrawati et al., 2017)

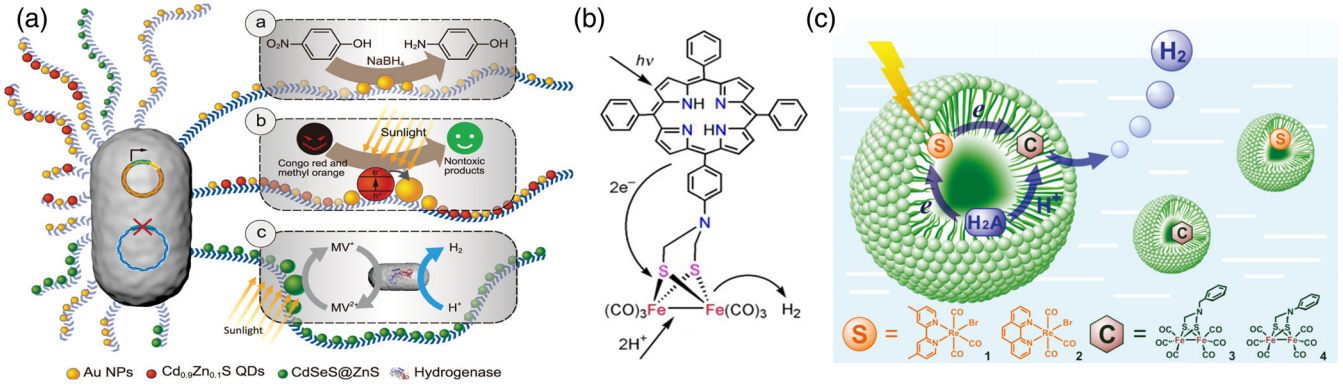

FIGURE 8 Typical hybrid catalyst delivery systems. (a) $Cd_{0.9}Se_{0.1}S$/CdSeS@ZnS QDs-anchored and hydrogenase-expressed curli fibers for hydrogen generation (Wang et al., 2019); (b) the hydrogenase mimic-porphyrin conjugation (Song et al., 2006); (c) the Re carbonyl compounds and hydrogenase mimic encapsulated micelle (Wang et al., 2010)

made a multigene plasmid based on ACEMBL expression system to produce hydrogenase for photocatalytic generation of H_2. $Cd_{0.9}Se_{0.1}S$/CdSeS@ZnS QDs can enhance the efficiency of light absorption in a wide range and increase the redox capability of hydrogenase by forming a Z-scheme-like structure, consequently significantly improving the hydrogen-producing performance of hydrogenase (Figure 8a).

Similarly, the mimics ($[Fe_2(CO)_6(m\text{-}adt)CH_2C_6H_5]$ and $[\{(m\text{-}SCH_2)_2N\}Fe_2(CO)_6]$ of hydrogenase ([FeFe] H_2ase) can also be sensitized by porphyrin (Figure 8b) (Song et al., 2006), CdTe QDs (Jian et al., 2013), and Re carbonyl compounds (Figure 8c) (Wang et al., 2010) for higher efficacy of hydrogen generation. Moreover, a sodium dodecyl sulfate micelle was used to encapsulate the hybrid system containing enzyme and photosensitizer to improve water solubility and achieve tumor-targeted delivery. Although reports and applications of this kind of hybrid system for gas therapy are still

rare, due to their excellent catalytic performances, we believe that the hybrid catalyst delivery strategy is promising for gas therapy in the future.

5 | CONCLUSIONS

Gas therapy has distinct advantages over traditional therapies. First, gas molecules are extremely small so that they can easily penetrate biomembranes to reach varied subcellular organelles such as mitochondria which are targeted points of NO, CO, H_2S, and H_2. Second, therapeutic gases are much safer than most toxic chemical drugs, inducing no or even overcoming drug resistance.

Though gas therapy boasts such advantages, how to efficiently transport therapeutic gases to the target is still of challenge. Some delivery strategies including physical gas encapsulation, artificial gas prodrugs and catalyzed gas production have been developed to improve the gas delivery efficiency. A large number of gas adsorbents have been developed, but their biomedical applications in therapeutic gas delivery are limited and thus need to be further explored. Many gas prodrugs have been designed for gas delivery, but the balance between their stability and controllability for gas release is worth investigating. The delivery of gas prodrugs is frequently used, but it is far from perfect as the delivery efficiency needs to be further improved and the prodrug structure of higher performance needs to be designed. Multifunctional nanocarriers play an important role in improving gas delivery performances. By comparison, the catalyst delivery strategy attracts more attention as no drug is needed as the carrier. Endogenous chemicals may be utilized as the substrate, enabling sustainable gas therapy, and the consumption of these chemicals as the substrate in gas production can also assist gas therapy. With catalyst delivery, the key is the development of powerful catalysts, especially those which can be excited by some stimuli sources with high tissue penetration capability such as X-ray and magnet field, which ensures high-efficacy therapy.

ACKNOWLEDGMENTS

This work was supported by the National Natural Science Foundation of China (51872188), Special Funds for the Development of Strategic Emerging Industries in Shenzhen (20180309154519685), SZU Top Ranking Project (860-00000210), and Center of Hydrogen Science, Shanghai Jiao Tong University, China.

CONFLICT OF INTEREST

The authors have declared no conflicts of interest for this article.

DATA AVAILABILITY STATEMENT

Data sharing is not applicable to this article as no new data were created or analyzed in this study.

AUTHOR CONTRIBUTIONS

Wanjun Gong: Conceptualization; writing - original draft. **Chao Xia:** Conceptualization; writing - original draft. **Qianjun He:** Conceptualization; funding acquisition; project administration; supervision; writing-review & editing.

ORCID

Wanjun Gong https://orcid.org/0000-0002-3099-032X
Chao Xia https://orcid.org/0000-0003-2886-6415
Qianjun He https://orcid.org/0000-0003-0689-8838

RELATED WIREs ARTICLE

Acoustically active liposome-nanobubble complexes for enhanced ultrasonic imaging and ultrasound-triggered drug delivery

REFERENCES

Allan, P. K., Wheatley, P. S., Aldous, D., Mohideen, M. I., Tang, C., Hriljac, J. A., Megson, I. L., Chapman, K. W., De Weireld, G., Vaesen, S., & Morris, R. E. (2012). Metal–organic frameworks for the storage and delivery of biologically active hydrogen sulfide. *Dalton Transactions*, *41*(14), 4060–4066. https://doi.org/10.1039/C2DT12069K

An, J., Hu, Y. G., Li, C., Hou, X. L., Cheng, K., Zhang, B., Zhang, R. Y., Li, D. Y., Liu, S. J., Liu, B., Zhu, D., & Zhao, Y. D. (2020). A pH/ultrasound dual-response biomimetic nanoplatform for nitric oxide gas-sonodynamic combined therapy and repeated ultrasound for relieving hypoxia. *Biomaterials*, *230*, 119636. https://doi.org/10.1016/j.biomaterials.2019.119636

Askes, S. H. C., Reddy, G. U., Wyrwa, R., Bonnet, S., & Schiller, A. (2017). Red light-triggered CO release from $Mn_2(CO)_{10}$ using triplet sensitization in polymer nonwoven fabrics. *Journal of the American Chemical Society*, *139*(43), 15292–15295. https://doi.org/10.1021/jacs.7b07427

Basudhar, D., Bharadwaj, G., Cheng, R. Y., Jain, S., Shi, S., Heinecke, J. L., Holland, R. J., Ridnour, L. A., Caceres, V. M., Spadari-Bratfisch, R. C., Paolocci, N., Velazquez-Martinez, C. A., Wink, D. A., & Miranda, K. M. (2013). Synthesis and chemical and biological comparison of nitroxyl- and nitric oxide-releasing diazeniumdiolate-based aspirin derivatives. *Journal of Medicinal Chemistry*, *56*(20), 7804–7820. https://doi.org/10.1021/jm400196q

Boakye-Yiadom, K. O., Kesse, S., Opoku-Damoah, Y., Filli, M. S., Aquib, M., Joelle, M. M. B., Farooq, M. A., Mavlyanova, R., Raza, F., Bavi, R., & Wang, B. (2019). Carbon dots: Applications in bioimaging and theranostics. *International Journal of Pharmaceutics*, *564*, 308–317. https://doi.org/10.1016/j.ijpharm.2019.04.055

Bohlender, C., Glaser, S., Klein, M., Weisser, J., Thein, S., Neugebauer, U., Popp, J., Wyrwa, R., & Schiller, A. (2014). Light-triggered CO release from nanoporous non-wovens. *Journal of Materials Chemistry B*, *2*(11), 1454–1463. https://doi.org/10.1039/c3tb21649g

Botov, S., Stamellou, E., Romanski, S., Guttentag, M., Alberto, R., Neudörfl, J.-M., Yard, B., & Schmalz, H.-G. (2013). Synthesis and performance of acyloxy-diene-$Fe(CO)_3$ complexes with variable chain lengths as enzyme-triggered carbon monoxide-releasing molecules. *Organometallics*, *32*(13), 3587–3594. https://doi.org/10.1021/om301233h

Carmona, F. J., Jimenez-Amezcua, I., Rojas, S., Romao, C. C., Navarro, J. A. R., Maldonado, C. R., & Barea, E. (2017). Aluminum doped MCM-41 nanoparticles as platforms for the dual encapsulation of a CO-releasing molecule and cisplatin. *Inorganic Chemistry*, *56*(17), 10474–10480. https://doi.org/10.1021/acs.inorgchem.7b01475

Carrington, S. J., Chakraborty, I., & Mascharak, P. K. (2013). Rapid CO release from a Mn(I) carbonyl complex derived from azopyridine upon exposure to visible light and its phototoxicity toward malignant cells. *Chemical Communications (Cambridge, England)*, *49*(96), 11254–11256. https://doi.org/10.1039/c3cc46558f

Chakraborty, I., Carrington, S. J., Hauser, J., Oliver, S. R. J., & Mascharak, P. K. (2015). Rapid eradication of human breast cancer cells through trackable light-triggered CO delivery by mesoporous silica nanoparticles packed with a designed photoCORM. *Chemistry of Materials*, *27*(24), 8387–8397. https://doi.org/10.1021/acs.chemmater.5b03859

Chakraborty, I., Carrington, S. J., & Mascharak, P. K. (2014). Design strategies to improve the sensitivity of photoactive metal carbonyl complexes (photoCORMs) to visible light and their potential as CO-donors to biological targets. *Accounts of Chemical Research*, *47*(8), 2603–2611. https://doi.org/10.1021/ar500172f

Chakraborty, I., Jimenez, J., & Mascharak, P. K. (2017). CO-induced apoptotic death of colorectal cancer cells by a luminescent photoCORM grafted on biocompatible carboxymethyl chitosan. *Chemical Communications (Cambridge, England)*, *53*(40), 5519–5522. https://doi.org/10.1039/c7cc02842c

Chandrawati, R., Chang, J. Y. H., Reina-Torres, E., Jumeaux, C., Sherwood, J. M., Stamer, W. D., Zelikin, A. N., Overby, D. R., & Stevens, M. M. (2017). Localized and controlled delivery of nitric oxide to the conventional outflow pathway via enzyme biocatalysis: Toward therapy for glaucoma. *Advanced Materials*, *29*(16), 1604932. https://doi.org/10.1002/adma.201604932

Chegaev, K., Rolando, B., Cortese, D., Gazzano, E., Buondonno, I., Lazzarato, L., Fanelli, M., Hattinger, C. M., Serra, M., Riganti, C., Fruttero, R., Ghigo, D., & Gasco, A. (2016). H_2S-donating doxorubicins may overcome cardiotoxicity and multidrug resistance. *Journal of Medicinal Chemistry*, *59*(10), 4881–4889. https://doi.org/10.1021/acs.jmedchem.6b00184

Chen, H., Cheng, Y., Tian, J., Yang, P., Zhang, X., Chen, Y., Hu, Y., & Wu, J. (2020). Dissolved oxygen from microalgae-gel patch promotes chronic wound healing in diabetes. *Science Advances*, *6*(20), eaba4311. https://doi.org/10.1126/sciadv.aba4311

Chen, H., He, W., & Guo, Z. (2014). An H_2O_2-responsive nanocarrier for dual-release of platinum anticancer drugs and O_2: Controlled release and enhanced cytotoxicity against cisplatin resistant cancer cells. *Chemical Communications*, *50*(68), 9714–9717. https://doi.org/10.1039/C4CC03385J

Chen, H., Tian, J., He, W., & Guo, Z. (2015). H_2O_2-activatable and O_2-evolving nanoparticles for highly efficient and selective photodynamic therapy against hypoxic tumor cells. *Journal of the American Chemical Society*, *137*(4), 1539–1547. https://doi.org/10.1021/ja511420n

Chen, J., Luo, H., Liu, Y., Zhang, W., Li, H., Luo, T., Zhang, K., Zhao, Y., & Liu, J. (2017). Oxygen-self-produced nanoplatform for relieving hypoxia and breaking resistance to sonodynamic treatment of pancreatic cancer. *ACS Nano*, *11*(12), 12849–12862. https://doi.org/10.1021/acsnano.7b08225

Chen, J., Sheng, D. D., Ying, T., Zhao, H. J., Zhang, J., Li, Y. X., Xu, H., & Chen, S. Y. (2020). MOFs-based nitric oxide therapy for tendon regeneration. *Nano-Micro Letters*, *13*(1), 23. https://doi.org/10.1007/s40820-020-00542-x

Chen, L., He, Q., Lei, M., Xiong, L., Shi, K., Tan, L., Jin, Z., Wang, T., & Qian, Z. (2017). Facile coordination-precipitation route to insoluble metal Roussin's black salts for NIR-responsive release of NO for anti-metastasis. *ACS Applied Materials and Interfaces*, *9*(42), 36473–36477. https://doi.org/10.1021/acsami.7b11325

Chen, L., Zhou, S.-F., Su, L., & Song, J. (2019). Gas-mediated cancer bioimaging and therapy. *ACS Nano*, *13*(10), 10887–10917. https://doi.org/10.1021/acsnano.9b04954

Chen, Q., Feng, L., Liu, J., Zhu, W., Dong, Z., Wu, Y., & Liu, Z. (2016). Intelligent albumin–MnO_2 nanoparticles as pH-/H_2O_2-responsive dissociable Nanocarriers to modulate tumor hypoxia for effective combination therapy. *Advanced Materials*, *28*(33), 7129–7136. https://doi.org/10.1002/adma.201601902

Chen, S., Takata, T., & Domen, K. (2017). Particulate photocatalysts for overall water splitting. *Nature Reviews Materials*, *2*(10), 17050. https://doi.org/10.1038/natrevmats.2017.50

Chen, W., Chen, M., Zang, Q., Wang, L., Tang, F., Han, Y., Yang, C., Deng, L., & Liu, Y. N. (2015). NIR light controlled release of caged hydrogen sulfide based on upconversion nanoparticles. *Chemical Communications (Cambridge, England)*, *51*(44), 9193–9196. https://doi.org/10.1039/c5cc02508g

Chen, Z., Yin, J.-J., Zhou, Y.-T., Zhang, Y., Song, L., Song, M., Hu, S., & Gu, N. (2012). Dual enzyme-like activities of iron oxide nanoparticles and their implication for diminishing cytotoxicity. *ACS Nano*, *6*(5), 4001–4012. https://doi.org/10.1021/nn300291r

Cheng, Y., Cheng, H., Jiang, C., Qiu, X., Wang, K., Huan, W., Yuan, A., Wu, J., & Hu, Y. (2015). Perfluorocarbon nanoparticles enhance reactive oxygen levels and tumour growth inhibition in photodynamic therapy. *Nature Communications*, *6*(1), 8785. https://doi.org/10.1038/ncomms9785

Choi, H. W., Kim, J., Kim, J., Kim, Y., Song, H. B., Kim, J. H., Kim, K., & Kim, W. J. (2016). Light-induced acid generation on a gatekeeper for smart nitric oxide delivery. *ACS Nano*, *10*(4), 4199–4208. https://doi.org/10.1021/acsnano.5b07483

Chuang, E. Y., Lin, C. C., Chen, K. J., Wan, D. H., Lin, K. J., Ho, Y. C., Lin, P. Y., & Sung, H. W. (2016). A FRET-guided, NIR-responsive bubble-generating liposomal system for in vivo targeted therapy with spatially and temporally precise controlled release. *Biomaterials*, *93*, 48–59. https://doi.org/10.1016/j.biomaterials.2016.03.040

Chung, M. F., Chen, K. J., Liang, H. F., Liao, Z. X., Chia, W. T., Xia, Y., & Sung, H. W. (2012). A liposomal system capable of generating CO_2 bubbles to induce transient cavitation, lysosomal rupturing, and cell necrosis. *Angewandte Chemie International Edition*, *51*(40), 10089–10093. https://doi.org/10.1002/anie.201205482

Chung, M. F., Liu, H. Y., Lin, K. J., Chia, W. T., & Sung, H. W. (2015). A pH-responsive carrier system that generates NO bubbles to trigger drug release and reverse P-glycoprotein-mediated multidrug resistance. *Angewandte Chemie International Edition*, *54*(34), 9890–9893. https://doi.org/10.1002/anie.201504444

Citi, V., Martelli, A., Testai, L., Marino, A., Breschi, M. C., & Calderone, V. (2014). Hydrogen sulfide releasing capacity of natural isothiocyanates: Is it a reliable explanation for the multiple biological effects of Brassicaceae? *Planta Medica*, *80*(8–9), 610–613. https://doi.org/10.1055/s-0034-1368591

Clark, J. E., Naughton, P., Shurey, S., Green, C. J., Johnson, T. R., Mann, B. E., Foresti, R., & Motterlini, R. (2003). Cardioprotective actions by a water-soluble carbon monoxide-releasing molecule. *Circulation Research*, *93*(2), e2–e8. https://doi.org/10.1161/01.RES.0000084381.86567.08

Day, J. J., Yang, Z., Chen, W., Pacheco, A., & Xian, M. (2016). Benzothiazole sulfinate: A water-soluble and slow-releasing sulfur dioxide donor. *ACS Chemical Biology*, *11*(6), 1647–1651. https://doi.org/10.1021/acschembio.6b00106

Diring, S., Carné-Sánchez, A., Zhang, J., Ikemura, S., Kim, C., Inaba, H., Kitagawa, S., & Furukawa, S. (2017). Light responsive metal–organic frameworks as controllable CO-releasing cell culture substrates. *Chemical Science*, *8*(3), 2381–2386. https://doi.org/10.1039/C6SC04824B

Diring, S., Wang, D. O., Kim, C., Kondo, M., Chen, Y., Kitagawa, S., Kamei, K., & Furukawa, S. (2013). Localized cell stimulation by nitric oxide using a photoactive porous coordination polymer platform. *Nature Communications*, *4*, 2684. https://doi.org/10.1038/ncomms3684

Dole, M., Wilson, F. R., & Fife, W. P. (1975). Hyperbaric hydrogen therapy: A possible treatment for cancer. *Science*, *190*(4210), 152–154. https://doi.org/10.1126/science.1166304

Eroy-Reveles, A. A., Leung, Y., Beavers, C. M., Olmstead, M. M., & Mascharak, P. K. (2008). Near-infrared light activated release of nitric oxide from designed photoactive manganese nitrosyls: Strategy, design, and potential as NO donors. *Journal of the American Chemical Society*, *130*(13), 4447–4458. https://doi.org/10.1021/ja710265j

Fan, J., He, N., He, Q., Liu, Y., Ma, Y., Fu, X., Liu, Y., Huang, P., & Chen, X. (2015). A novel self-assembled sandwich nanomedicine for NIR-responsive release of NO. *Nanoscale*, *7*(47), 20055–20062. https://doi.org/10.1039/c5nr06630a

Fan, J., He, Q., Liu, Y., Zhang, F., Yang, X., Wang, Z., Lu, N., Fan, W., Lin, L., Niu, G., He, N., Song, J., & Chen, X. (2016). Light-responsive biodegradable nanomedicine overcomes multidrug resistance via NO-enhanced chemosensitization. *ACS Applied Materials and Interfaces*, *8*(22), 13804–13811. https://doi.org/10.1021/acsami.6b03737

Fan, M., Wen, Y., Ye, D., Jin, Z., Zhao, P., Chen, D., Lu, X., & He, Q. (2019). Acid-responsive H_2-releasing 2D MgB_2 nanosheet for therapeutic synergy and side effect attenuation of gastric cancer chemotherapy. *Advanced Healthcare Materials*, *8*(13), e1900157. https://doi.org/10.1002/adhm.201900157

Fan, W., Bu, W., Zhang, Z., Shen, B., Zhang, H., He, Q., Ni, D., Cui, Z., Zhao, K., Bu, J., Du, J., Liu, J., & Shi, J. (2015). X-ray radiation-controlled NO-release for on-demand depth-independent hypoxic radiosensitization. *Angewandte Chemie International Edition*, *54*(47), 14026–14030. https://doi.org/10.1002/anie.201504536

Feng, Q., Zhang, W., Yang, X., Li, Y., Hao, Y., Zhang, H., Hou, L., & Zhang, Z. (2018). pH/ultrasound dual-responsive gas generator for ultrasound imaging-guided therapeutic inertial cavitation and sonodynamic therapy. *Advanced Healthcare Materials*, *7*(5), 1700957. https://doi.org/10.1002/adhm.201700957

Foster, J. C., Radzinski, S. C., Zou, X., Finkielstein, C. V., & Matson, J. B. (2017). H_2S-releasing polymer micelles for studying selective cell toxicity. *Molecular Pharmaceutics*, *14*(4), 1300–1306. https://doi.org/10.1021/acs.molpharmaceut.6b01117

Fujimoto, H., Ohno, M., Ayabe, S., Kobayashi, H., Ishizaka, N., Kimura, H., Yoshida, K., & Nagai, R. (2004). Carbon monoxide protects against cardiac ischemia–reperfusion injury in vivo via MAPK and Akt–eNOS pathways. *Arteriosclerosis, Thrombosis, and Vascular Biology*, *24*(10), 1848–1853. https://doi.org/10.1161/01.ATV.0000142364.85911.0e

Gao, S., Zheng, P., Li, Z., Feng, X., Yan, W., Chen, S., Guo, W., Liu, D., Yang, X., Wang, S., Liang, X.-J., & Zhang, J. (2018). Biomimetic O_2 – Evolving metal-organic framework nanoplatform for highly efficient photodynamic therapy against hypoxic tumor. *Biomaterials*, *178*, 83–94. https://doi.org/10.1016/j.biomaterials.2018.06.007

Garcia, J. V., Yang, J., Shen, D., Yao, C., Li, X., Wang, R., Stucky, G. D., Zhao, D., Ford, P. C., & Zhang, F. (2012). NIR-triggered release of caged nitric oxide using upconverting nanostructured materials. *Small*, *8*(24), 3800–3805. https://doi.org/10.1002/smll.201201213

Gu, R., Wang, L., Huang, X., Zhang, J., Ou, C., Si, W., Yu, J., Wang, W., & Dong, X. (2020). pH/glutathione-responsive release of SO_2 induced superoxide radical accumulation for gas therapy of cancer. *Chemical Communications (Cambridge, England)*, *56*(94), 14865–14868. https://doi.org/10.1039/d0cc06826h

Guan, Q., Zhou, L.-L., Li, Y.-A., & Dong, Y.-B. (2019). A nanoscale metal–organic framework for combined photodynamic and starvation therapy in treating breast tumors. *Chemical Communications*, *55*(99), 14898–14901. https://doi.org/10.1039/C9CC07510K

Guo, R. R., Tian, Y., Wang, Y. J., & Yang, W. L. (2017). Near-infrared laser-triggered nitric oxide nanogenerators for the reversal of multidrug resistance in cancer. *Advanced Functional Materials*, *27*(13), 1606398. https://doi.org/10.1002/adfm.201606398

Haikal, R. R., Hua, C., Perry, J. J., O'Nolan, D., Syed, I., Kumar, A., Chester, A. H., Zaworotko, M. J., Yacoub, M. H., & Alkordi, M. H. (2017). Controlling the uptake and regulating the release of nitric oxide in microporous solids. *ACS Applied Materials and Interfaces*, *9*(50), 43520–43528. https://doi.org/10.1021/acsami.7b15095

Han, H. D., Jeon, Y. W., Kwon, H. J., Jeon, H. N., Byeon, Y., Lee, C. O., Cho, S. H., & Shin, B. C. (2015). Therapeutic efficacy of doxorubicin delivery by a CO_2 generating liposomal platform in breast carcinoma. *Acta Biomaterialia*, *24*, 279–285. https://doi.org/10.1016/j.actbio.2015.06.019

Hasegawa, U., & van der Vlies, A. J. (2014). Design and synthesis of polymeric hydrogen sulfide donors. *Bioconjugate Chemistry*, *25*(7), 1290–1300. https://doi.org/10.1021/bc500150s

He, Q., Kiesewetter, D. O., Qu, Y., Fu, X., Fan, J., Huang, P., Liu, Y., Zhu, G., Liu, Y., Qian, Z., & Chen, X. (2015). NIR-responsive on-demand release of CO from metal carbonyl-caged graphene oxide nanomedicine. *Advanced Materials*, *27*(42), 6741–6746. https://doi.org/10.1002/adma.201502762

He, T., Qin, X., Jiang, C., Jiang, D., Lei, S., Lin, J., Zhu, W. G., Qu, J., & Huang, P. (2020). Tumor pH-responsive metastable-phase manganese sulfide nanotheranostics for traceable hydrogen sulfide gas therapy primed chemodynamic therapy. *Theranostics*, *10*(6), 2453–2462. https://doi.org/10.7150/thno.42981

He, Y., Zhang, B., Chen, Y., Jin, Q., Wu, J., Yan, F., & Zheng, H. (2017). Image-guided hydrogen gas delivery for protection from myocardial ischemia–reperfusion injury via microbubbles. *ACS Applied Materials and Interfaces*, *9*(25), 21190–21199. https://doi.org/10.1021/acsami.7b05346

Heilman, B. J., St John, J., Oliver, S. R., & Mascharak, P. K. (2012). Light-triggered eradication of *Acinetobacter baumannii* by means of NO delivery from a porous material with an entrapped metal nitrosyl. *Journal of the American Chemical Society*, *134*(28), 11573–11582. https://doi.org/10.1021/ja3022736

Hou, J., Pan, Y., Zhu, D., Fan, Y., Feng, G., Wei, Y., Wang, H., Qin, K., Zhao, T., Yang, Q., Zhu, Y., Che, Y., Liu, Y., Cheng, J., Kong, D., Wang, P. G., Shen, J., & Zhao, Q. (2019). Targeted delivery of nitric oxide via a 'bump-and-hole'-based enzyme-prodrug pair. *Nature Chemical Biology*, *15*(2), 151–160. https://doi.org/10.1038/s41589-018-0190-5

Huang, S.-L., Kee Patrick, H., Kim, H., Moody Melanie, R., Chrzanowski Stephen, M., MacDonald Robert, C., & McPherson David, D. (2009). Nitric oxide-loaded echogenic liposomes for nitric oxide delivery and inhibition of intimal hyperplasia. *Journal of the American College of Cardiology*, *54*(7), 652–659. https://doi.org/10.1016/j.jacc.2009.04.039

Huo, M., Wang, L., Zhang, L., Wei, C., Chen, Y., & Shi, J. (2020). Photosynthetic tumor oxygenation by photosensitizer-containing *Cyanobacteria* for enhanced photodynamic therapy. *Angewandte Chemie International Edition*, *59*(5), 1906–1913. https://doi.org/10.1002/anie.201912824

Jang, H. J., Jeong, E. J., & Lee, K. Y. (2018). Carbon dioxide-generating PLG nanoparticles for controlled anti-cancer drug delivery. *Pharmaceutical Research*, *35*(3), 59. https://doi.org/10.1007/s11095-018-2359-8

Ji, X., De La Cruz, L. K. C., Pan, Z., Chittavong, V., & Wang, B. (2017). pH-sensitive metal-free carbon monoxide prodrugs with tunable and predictable release rates. *Chemical Communications (Cambridge, England)*, *53*(69), 9628–9631. https://doi.org/10.1039/c7cc04866a

Ji, X., El-Labbad, E. M., Ji, K., Lasheen, D. S., Serya, R. A., Abouzid, K. A., & Wang, B. (2017). Click and release: SO_2 prodrugs with tunable release rates. *Organic Letters*, *19*(4), 818–821. https://doi.org/10.1021/acs.orglett.6b03805

Ji, X., Ji, K., Chittavong, V., Yu, B., Pan, Z., & Wang, B. (2017). An esterase-activated click and release approach to metal-free CO-prodrugs. *Chemical Communications (Cambridge, England)*, *53*(59), 8296–8299. https://doi.org/10.1039/c7cc03832a

Ji, X., Zhou, C., Ji, K., Aghoghovbia, R. E., Pan, Z., Chittavong, V., Ke, B., & Wang, B. (2016). Click and release: A chemical strategy toward developing gasotransmitter prodrugs by using an intramolecular Diels–Alder reaction. *Angewandte Chemie International Edition*, *55*(51), 15846–15851. https://doi.org/10.1002/anie.201608732

Jia, X., Zhang, Y., Zou, Y., Wang, Y., Niu, D., He, Q., Huang, Z., Zhu, W., Tian, H., Shi, J., & Li, Y. (2018). Dual intratumoral redox/enzyme-responsive NO-releasing nanomedicine for the specific, high-efficacy, and low-toxic cancer therapy. *Advanced Materials*, *30*(30), 1704490. https://doi.org/10.1002/adma.201704490

Jian, J.-X., Liu, Q., Li, Z.-J., Wang, F., Li, X.-B., Li, C.-B., Liu, B., Meng, Q.-Y., Chen, B., & Feng, K. (2013). Chitosan confinement enhances hydrogen photogeneration from a mimic of the diiron subsite of [FeFe]-hydrogenase. *Nature Communications*, *4*(1), 1–9. https://doi.org/10.1038/ncomms3695

Jin, Z., Wen, Y., Hu, Y., Chen, W., Zheng, X., Guo, W., Wang, T., Qian, Z., Su, B. L., & He, Q. (2017). MRI-guided and ultrasound-triggered release of NO by advanced nanomedicine. *Nanoscale*, *9*(10), 3637–3645. https://doi.org/10.1039/c7nr00231a

Jin, Z., Wen, Y., Xiong, L., Yang, T., Zhao, P., Tan, L., Wang, T., Qian, Z., Su, B. L., & He, Q. (2017). Intratumoral H_2O_2-triggered release of CO from a metal carbonyl-based nanomedicine for efficient CO therapy. *Chemical Communications (Cambridge, England)*, *53*(40), 5557–5560. https://doi.org/10.1039/c7cc01576c

Jin, Z., Zhao, P., Zhang, J., Yang, T., Zhou, G., Zhang, D., Wang, T., & He, Q. (2018). Intelligent metal carbonyl metal-organic framework nanocomplex for fluorescent traceable H_2O_2-triggered CO delivery. *Chemistry*, *24*(45), 11667–11674. https://doi.org/10.1002/chem.201801407

Kang, Y., Kim, J., Park, J., Lee, Y. M., Saravanakumar, G., Park, K. M., Choi, W., Kim, K., Lee, E., Kim, C., & Kim, W. J. (2019). Tumor vasodilation by N-heterocyclic carbene-based nitric oxide delivery triggered by high-intensity focused ultrasound and enhanced drug homing to tumor sites for anti-cancer therapy. *Biomaterials*, *217*, 119297. https://doi.org/10.1016/j.biomaterials.2019.119297

Kao, P. T., Lee, I. J., Liau, I., & Yeh, C. S. (2017). Controllable NO release from $Cu_{1.6}S$ nanoparticle decomposition of S-nitrosoglutathiones following photothermal disintegration of polymersomes to elicit cerebral vasodilatory activity. *Chemical Science*, *8*(1), 291–297. https://doi.org/10.1039/c6sc02774a

Kawahara, B., Gao, L., Cohn, W., Whitelegge, J. P., Sen, S., Janzen, C., & Mascharak, P. K. (2020). Diminished viability of human ovarian cancer cells by antigen-specific delivery of carbon monoxide with a family of photoactivatable antibody-photoCORM conjugates. *Chemical Science*, *11*(2), 467–473. https://doi.org/10.1039/C9SC03166A

Kawahara, B., Moller, T., Hu-Moore, K., Carrington, S., Faull, K. F., Sen, S., & Mascharak, P. K. (2017). Attenuation of antioxidant capacity in human breast cancer cells by carbon monoxide through inhibition of cystathionine beta-synthase activity: Implications in chemotherapeutic drug sensitivity. *Journal of Medicinal Chemistry*, *60*(19), 8000–8010. https://doi.org/10.1021/acs.jmedchem.7b00476

Kim, I., Han, E. H., Bang, W.-Y., Ryu, J., Min, J.-Y., Nam, H. C., Park, W. H., Chung, Y.-H., & Lee, E. (2018). Supramolecular carbon monoxide-releasing peptide hydrogel patch. *Advanced Functional Materials*, *28*(47), 1803051. https://doi.org/10.1002/adfm.201803051

Kodama, R., Sumaru, K., Morishita, K., Kanamori, T., Hyodo, K., Kamitanaka, T., Morimoto, M., Yokojima, S., Nakamura, S., & Uchida, K. (2015). A diarylethene as the SO_2 gas generator upon UV irradiation. *Chemical Communications (Cambridge, England)*, *51*(9), 1736–1738. https://doi.org/10.1039/c4cc07790c

Kong, L., Chen, C. R., Mou, F. Z., Feng, Y. Z., You, M., Yin, Y. X., & Guan, J. G. (2019). Magnesium particles coated with mesoporous nanoshells as sustainable therapeutic-hydrogen suppliers to scavenge continuously generated hydroxyl radicals in long term. *Particle & Particle Systems Characterization*, *36*(2), 1800424. https://doi.org/10.1002/ppsc.201800424

Kou, Z., Zhao, P., Wang, Z., Jin, Z., Chen, L., Su, B. L., & He, Q. (2019). Acid-responsive H_2-releasing Fe nanoparticles for safe and effective cancer therapy. *Journal of Materials Chemistry B*, *7*(17), 2759–2765. https://doi.org/10.1039/c9tb00338j

Krathumkhet, N., Sabrina, Imae, T., & Krafft, M. P. (2021). Nitric oxide gas in carbon nanohorn/fluorinated dendrimer/fluorinated poly(ethylene glycol)-based hierarchical nanocomposites as therapeutic nanocarriers. *ACS Applied Bio Materials*, *4*(3), 2591–2600. https://doi.org/10.1021/acsabm.0c01577

Kunz, P. C., Meyer, H., Barthel, J., Sollazzo, S., Schmidt, A. M., & Janiak, C. (2013). Metal carbonyls supported on iron oxide nanoparticles to trigger the CO-gasotransmitter release by magnetic heating. *Chemical Communications (Cambridge, England)*, *49*(43), 4896–4898. https://doi.org/10.1039/c3cc41411f

Lee, H. J., Kim, D. E., Park, D. J., Choi, G. H., Yang, D. N., Heo, J. S., & Lee, S. C. (2016). pH-responsive mineralized nanoparticles as stable nanocarriers for intracellular nitric oxide delivery. *Colloids and Surfaces B: Biointerfaces*, *146*, 1–8. https://doi.org/10.1016/j.colsurfb.2016.05.039

Li, S., Liu, R., Jiang, X., Qiu, Y., Song, X., Huang, G., Fu, N., Lin, L., Song, J., Chen, X., & Yang, H. (2019). Near-infrared light-triggered sulfur dioxide gas therapy of cancer. *ACS Nano*, *13*(2), 2103–2113. https://doi.org/10.1021/acsnano.8b08700

Li, S.-Y., Cheng, H., Xie, B.-R., Qiu, W.-X., Zeng, J.-Y., Li, C.-X., Wan, S.-S., Zhang, L., Liu, W.-L., & Zhang, X.-Z. (2017). Cancer cell membrane camouflaged cascade bioreactor for cancer targeted starvation and photodynamic therapy. *ACS Nano*, *11*(7), 7006–7018. https://doi.org/10.1021/acsnano.7b02533

Li, W. P., Su, C. H., Tsao, L. C., Chang, C. T., Hsu, Y. P., & Yeh, C. S. (2016). Controllable CO release following near-infrared light-induced cleavage of iron carbonyl derivatized Prussian blue nanoparticles for CO-assisted synergistic treatment. *ACS Nano*, *10*(12), 11027–11036. https://doi.org/10.1021/acsnano.6b05858

Li, Y. H., Guo, M., Shi, S. W., Zhang, Q. L., Yang, S. P., & Liu, J. G. (2017). A ruthenium-nitrosyl-functionalized nanoplatform for the targeting of liver cancer cells and NIR-light-controlled delivery of nitric oxide combined with photothermal therapy. *Journal of Materials Chemistry B*, *5*(38), 7831–7838. https://doi.org/10.1039/c7tb02059g

Liang, S., Deng, X., Chang, Y., Sun, C., Shao, S., Xie, Z., Xiao, X., Ma, P. a., Zhang, H., Cheng, Z., & Lin, J. (2019). Intelligent hollow Pt-CuS Janus architecture for synergistic catalysis-enhanced sonodynamic and photothermal cancer therapy. *Nano Letters*, *19*(6), 4134–4145. https://doi.org/10.1021/acs.nanolett.9b01595

Liu, C., Kurokawa, R., Fujino, M., Hirano, S., Sato, B., & Li, X. K. (2014). Estimation of the hydrogen concentration in rat tissue using an air-tight tube following the administration of hydrogen via various routes. *Scientific Reports*, *4*(1), 1–11. https://doi.org/10.1038/srep05485

Liu, T., Zhang, N., Wang, Z., Wu, M., Chen, Y., Ma, M., Chen, H., & Shi, J. (2017). Endogenous catalytic generation of O_2 bubbles for in situ ultrasound-guided high intensity focused ultrasound ablation. *ACS Nano*, *11*(9), 9093–9102. https://doi.org/10.1021/acsnano.7b03772

Long, L., Jiang, X., Wang, X., Xiao, Z., & Liu, X. (2013). Water-soluble diiron hexacarbonyl complex as a CO-RM: Controllable CO-releasing, releasing mechanism and biocompatibility. *Dalton Transactions*, *42*(44), 15663–15669. https://doi.org/10.1039/c3dt51281a

Lu, Q., Lu, T., Xu, M., Yang, L., Song, Y., & Li, N. (2020). SO_2 prodrug doped nanorattles with extra-high drug payload for "collusion inside and outside" photothermal/pH triggered-gas therapy. *Biomaterials*, *257*, 120236. https://doi.org/10.1016/j.biomaterials.2020.120236

Ma, M., Noei, H., Mienert, B., Niesel, J., Bill, E., Muhler, M., Fischer, R. A., Wang, Y., Schatzschneider, U., & Metzler-Nolte, N. (2013). Iron metal–organic frameworks MIL-88B and NH2-MIL-88B for the loading and delivery of the gasotransmitter carbon monoxide. *Chemistry – A European Journal*, *19*(21), 6785–6790. https://doi.org/10.1002/chem.201201743

Ma, R., Wu, Q., Si, T., Chang, S., & Xu, R. X. (2017). Oxygen and indocyanine green loaded microparticles for dual-mode imaging and sonodynamic treatment of cancer cells. *Ultrasonics Sonochemistry*, *39*, 197–207. https://doi.org/10.1016/j.ultsonch.2017.03.019

Ma, W., Chen, X., Fu, L., Zhu, J., Fan, M., Chen, J., Yang, C., Yang, G., Wu, L., Mao, G., Yang, X., Mou, X., Gu, Z., & Cai, X. (2020). Ultra-efficient antibacterial system based on photodynamic therapy and CO gas therapy for synergistic antibacterial and ablation biofilms. *ACS Applied Materials and Interfaces*, *12*(20), 22479–22491. https://doi.org/10.1021/acsami.0c01967

Malwal, S. R., Sriram, D., Yogeeswari, P., Konkimalla, V. B., & Chakrapani, H. (2012). Design, synthesis, and evaluation of thiol-activated sources of sulfur dioxide (SO(2)) as antimycobacterial agents. *Journal of Medicinal Chemistry*, *55*(1), 553–557. https://doi.org/10.1021/jm201023g

Mamaghani, A. H., Haghighat, F., & Lee, C.-S. (2017). Photocatalytic oxidation technology for indoor environment air purification: The state-of-the-art. *Applied Catalysis B*, *203*, 247–269. https://doi.org/10.1016/j.apcatb.2016.10.037

Martelli, A., Testai, L., Citi, V., Marino, A., Bellagambi, F. G., Ghimenti, S., Breschi, M. C., & Calderone, V. (2014). Pharmacological characterization of the vascular effects of aryl isothiocyanates: Is hydrogen sulfide the real player? *Vascular Pharmacology*, *60*(1), 32–41. https://doi.org/10.1016/j.vph.2013.11.003

Martelli, A., Testai, L., Citi, V., Marino, A., Pugliesi, I., Barresi, E., Nesi, G., Rapposelli, S., Taliani, S., Da Settimo, F., Breschi, M. C., & Calderone, V. (2013). Arylthioamides as H_2S donors: L-Cysteine-activated releasing properties and vascular effects in vitro and in vivo. *ACS Medicinal Chemistry Letters*, *4*(10), 904–908. https://doi.org/10.1021/ml400239a

Matson, J. B., Webber, M. J., Tamboli, V. K., Weber, B., & Stupp, S. I. (2012). A peptide-based material for therapeutic carbon monoxide delivery. *Soft Matter*, *8*(25), 2689–2692. https://doi.org/10.1039/C2SM25785H

McKinlay, A. C., Eubank, J. F., Wuttke, S., Xiao, B., Wheatley, P. S., Bazin, P., Lavalley, J. C., Daturi, M., Vimont, A., De Weireld, G., Horcajada, P., Serre, C., & Morris, R. E. (2013). Nitric oxide adsorption and delivery in flexible MIL-88(Fe) metal–organic frameworks. *Chemistry of Materials*, *25*(9), 1592–1599. https://doi.org/10.1021/cm304037x

McKinlay, A. C., Xiao, B., Wragg, D. S., Wheatley, P. S., Megson, I. L., & Morris, R. E. (2008). Exceptional behavior over the whole adsorption–storage–delivery cycle for NO in porous metal organic frameworks. *Journal of the American Chemical Society*, *130*(31), 10440–10444. https://doi.org/10.1021/ja801997r

Meng, J., Jin, Z., Zhao, P., Zhao, B., Fan, M., & He, Q. (2020). A multistage assembly/disassembly strategy for tumor-targeted CO delivery. *Science Advances*, *6*(20), eaba1362. https://doi.org/10.1126/sciadv.aba1362

Meyer, H., Brenner, M., Höfert, S.-P., Knedel, T.-O., Kunz, P. C., Schmidt, A. M., Hamacher, A., Kassack, M. U., & Janiak, C. (2016). Synthesis of oxime-based CO-releasing molecules, CORMs and their immobilization on maghemite nanoparticles for magnetic-field induced CO release. *Dalton Transactions*, *45*(18), 7605–7615. https://doi.org/10.1039/c5dt04888e

Meyer, H., Winkler, F., Kunz, P., Schmidt, A. M., Hamacher, A., Kassack, M. U., & Janiak, C. (2015). Stabilizing alginate confinement and polymer coating of CO-releasing molecules supported on iron oxide nanoparticles to trigger the CO release by magnetic heating. *Inorganic Chemistry*, *54*(23), 11236–11246. https://doi.org/10.1021/acs.inorgchem.5b01675

Mikami, Y., Shibuya, N., Kimura, Y., Nagahara, N., Ogasawara, Y., & Kimura, H. (2011). Thioredoxin and dihydrolipoic acid are required for 3-mercaptopyruvate sulfurtransferase to produce hydrogen sulfide. *The Biochemical Journal*, *439*(3), 479–485. https://doi.org/10.1042/BJ20110841

Min, K. H., Min, H. S., Lee, H. J., Park, D. J., Yhee, J. Y., Kim, K., Kwon, I. C., Jeong, S. Y., Silvestre, O. F., Chen, X., Hwang, Y. S., Kim, E. C., & Lee, S. C. (2015). pH-controlled gas-generating mineralized nanoparticles: A theranostic agent for ultrasound imaging and therapy of cancers. *ACS Nano*, *9*(1), 134–145. https://doi.org/10.1021/nn506210a

Motterlini, R., & Otterbein, L. E. (2010). The therapeutic potential of carbon monoxide. *Nature Reviews Drug Discovery*, *9*(9), 728–743. https://doi.org/10.1038/nrd3228

Mowbray, M., Tan, X., Wheatley, P. S., Morris, R. E., & Weller, R. B. (2008). Topically applied nitric oxide induces T-lymphocyte infiltration in human skin, but minimal inflammation. *Journal of Investigative Dermatology*, *128*(2), 352–360. https://doi.org/10.1038/sj.jid.5701096

Ohsawa, I., Ishikawa, M., Takahashi, K., Watanabe, M., Nishimaki, K., Yamagata, K., Katsura, K.-I., Katayama, Y., Asoh, S., & Ohta, S. (2007). Hydrogen acts as a therapeutic antioxidant by selectively reducing cytotoxic oxygen radicals. *Nature Medicine*, *13*(6), 688–694. https://doi.org/10.1038/nm1577

Palao, E., Slanina, T., Muchova, L., Solomek, T., Vitek, L., & Klan, P. (2016). Transition-metal-free CO-releasing BODIPY derivatives activatable by visible to NIR light as promising bioactive molecules. *Journal of the American Chemical Society*, *138*(1), 126–133. https://doi.org/10.1021/jacs.5b10800

Palmer, R. M. J., Ferrige, A. G., & Moncada, S. (1987). Nitric oxide release accounts for the biological activity of endothelium-derived relaxing factor. *Nature*, *327*(6122), 524–526. https://doi.org/10.1038/327524a0

Pan, Z., Chittavong, V., Li, W., Zhang, J., Ji, K., Zhu, M., Ji, X., & Wang, B. (2017). Organic CO prodrugs: Structure-CO-release rate relationship studies. *Chemistry*, *23*(41), 9838–9845. https://doi.org/10.1002/chem.201700936

Park, J., Song, H., Kim, Y., Eun, B., Kim, Y., Bae, D. Y., Park, S., Rhee, Y. M., Kim, W. J., Kim, K., & Lee, E. (2015). N-heterocyclic carbene nitric oxide radicals. *Journal of the American Chemical Society*, *137*(14), 4642–4645. https://doi.org/10.1021/jacs.5b01976

Pinto, M. L., Fernandes, A. C., Antunes, F., Pires, J., & Rocha, J. (2016). Storage and delivery of nitric oxide by microporous titanosilicate ETS-10 and Al and Ga substituted analogues. *Microporous and Mesoporous Materials*, *229*, 83–89. https://doi.org/10.1016/j.micromeso.2016.04.021

Pinto, M. L., Fernandes, A. C., Rocha, J., Ferreira, A., Antunes, F., & Pires, J. (2014). Microporous titanosilicates Cu^{2+}- and Co^{2+}-ETS-4 for storage and slow release of therapeutic nitric oxide. *Journal of Materials Chemistry B*, *2*(2), 224–230. https://doi.org/10.1039/C3TB20929F

Pinto, M. L., Rocha, J., Gomes, J. R. B., & Pires, J. (2011). Slow release of NO by microporous titanosilicate ETS-4. *Journal of the American Chemical Society*, *133*(16), 6396–6402. https://doi.org/10.1021/ja200663e

Pinto, R. V., Wang, S., Tavares, S. R., Pires, J., Antunes, F., Vimont, A., Clet, G., Daturi, M., Maurin, G., Serre, C., & Pinto, M. L. (2020). Tuning cellular biological functions through the controlled release of NO from a porous Ti-MOF. *Angewandte Chemie International Edition*, *59*(13), 5135–5143. https://doi.org/10.1002/anie.201913135

Popova, M., Lazarus, L. S., Ayad, S., Benninghoff, A. D., & Berreau, L. M. (2018). Visible-light-activated quinolone carbon-monoxide-releasing molecule: Prodrug and albumin-assisted delivery enables anticancer and potent anti-inflammatory effects. *Journal of the American Chemical Society*, *140*(30), 9721–9729. https://doi.org/10.1021/jacs.8b06011

Roger, T., Raynaud, F., Bouillaud, F., Ransy, C., Simonet, S., Crespo, C., Bourguignon, M. P., Villeneuve, N., Vilaine, J. P., Artaud, I., & Galardon, E. (2013). New biologically active hydrogen sulfide donors. *Chembiochem*, *14*(17), 2268–2271. https://doi.org/10.1002/cbic.201300552

Romanski, S., Rücker, H., Stamellou, E., Guttentag, M., Neudörfl, J.-M., Alberto, R., Amslinger, S., Yard, B., & Schmalz, H.-G. (2012). Iron dienylphosphate tricarbonyl complexes as water-soluble enzyme-triggered CO-releasing molecules (ET-CORMs). *Organometallics*, *31*(16), 5800–5809. https://doi.org/10.1021/om300359a

Ryter, S. W., & Otterbein, L. E. (2004). Carbon monoxide in biology and medicine. *BioEssays*, *26*(3), 270–280. https://doi.org/10.1002/bies.20005

Sakla, R., & Jose, D. A. (2018). Vesicles functionalized with a CO-releasing molecule for light-induced CO delivery. *ACS Applied Materials and Interfaces*, *10*(16), 14214–14220. https://doi.org/10.1021/acsami.8b03310

Song, G., Liang, C., Yi, X., Zhao, Q., Cheng, L., Yang, K., & Liu, Z. (2016). Perfluorocarbon-loaded hollow Bi_2Se_3 nanoparticles for timely supply of oxygen under near-infrared light to enhance the radiotherapy of cancer. *Advanced Materials*, *28*(14), 2716–2723. https://doi.org/10.1002/adma.201504617

Song, L.-C., Tang, M.-Y., Su, F.-H., & Hu, Q.-M. (2006). A biomimetic model for the active site of iron-only hydrogenases covalently bonded to a porphyrin photosensitizer. *Angewandte Chemie International Edition*, *45*(7), 1130–1133. https://doi.org/10.1002/anie.200503602

Song, X., Feng, L., Liang, C., Yang, K., & Liu, Z. (2016). Ultrasound triggered tumor oxygenation with oxygen-shuttle nanoperfluorocarbon to overcome hypoxia-associated resistance in cancer therapies. *Nano Letters*, *16*(10), 6145–6153. https://doi.org/10.1021/acs.nanolett.6b02365

Stasko, N. A., & Schoenfisch, M. H. (2006). Dendrimers as a scaffold for nitric oxide release. *Journal of the American Chemical Society*, *128*(25), 8265–8271. https://doi.org/10.1021/ja060875z

Steiger, A. K., Yang, Y., Royzen, M., & Pluth, M. D. (2017). Bio-orthogonal "click-and-release" donation of caged carbonyl sulfide (COS) and hydrogen sulfide (H_2S). *Chemical Communications (Cambridge, England)*, *53*(8), 1378–1380. https://doi.org/10.1039/c6cc09547j

Sun, R., Liu, X., Li, G., Wang, H., Luo, Y., Huang, G., Wang, X., Zeng, G., Liu, Z., & Wu, S. (2020). Photoactivated H_2 nanogenerator for enhanced chemotherapy of bladder cancer. *ACS Nano*, *14*(7), 8135–8148. https://doi.org/10.1021/acsnano.0c01300

Sun, X., Kong, B., Wang, W., Chandran, P., Selomulya, C., Zhang, H., Zhu, K., Liu, Y., Yang, W., Guo, C., Zhao, D., & Wang, C. (2015). Mesoporous silica nanoparticles for glutathione-triggered long-range and stable release of hydrogen sulfide. *Journal of Materials Chemistry B*, *3*(21), 4451–4457. https://doi.org/10.1039/c5tb00354g

Tang, W., Fan, W., Wang, Z., Zhang, W., Zhou, S., Liu, Y., Yang, Z., Shao, E., Zhang, G., Jacobson, O., Shan, L., Tian, R., Cheng, S., Lin, L., Dai, Y., Shen, Z., Niu, G., Xie, J., & Chen, X. (2018). Acidity/reducibility dual-responsive hollow mesoporous organosilica nanoplatforms for tumor-specific self-assembly and synergistic therapy. *ACS Nano*, *12*(12), 12269–12283. https://doi.org/10.1021/acsnano.8b06058

Tew, K. D., Manevich, Y., Grek, C., Xiong, Y., Uys, J., & Townsend, D. M. (2011). The role of glutathione S-transferase P in signaling pathways and S-glutathionylation in cancer. *Free Radical Biology and Medicine*, *51*(2), 299–313. https://doi.org/10.1016/j.freeradbiomed.2011.04.013

Thommes, M. (2010). Physical adsorption characterization of nanoporous materials. *Chemie Ingenieur Technik*, *82*(7), 1059–1073. https://doi.org/10.1002/cite.201000064

Thommes, M., & Cychosz, K. A. (2014). Physical adsorption characterization of nanoporous materials: Progress and challenges. *Adsorption-Journal of the International Adsorption Society*, *20*(2–3), 233–250. https://doi.org/10.1007/s10450-014-9606-z

van der Vlies, A. J., Inubushi, R., Uyama, H., & Hasegawa, U. (2016). Polymeric framboidal nanoparticles loaded with a carbon monoxide donor via phenylboronic acid-catechol complexation. *Bioconjugate Chemistry*, *27*(6), 1500–1508. https://doi.org/10.1021/acs.bioconjchem.6b00135

Vong, L. B., & Nagasaki, Y. (2020). Nitric oxide nano-delivery systems for cancer therapeutics: Advances and challenges. *Antioxidants (Basel)*, *9*(9), 791. https://doi.org/10.3390/antiox9090791

Wan, W.-L., Lin, Y.-J., Chen, H.-L., Huang, C.-C., Shih, P.-C., Bow, Y.-R., Chia, W.-T., & Sung, H.-W. (2017). In situ nanoreactor for photosynthesizing H_2 gas to mitigate oxidative stress in tissue inflammation. *Journal of the American Chemical Society*, *139*(37), 12923–12926. https://doi.org/10.1021/jacs.7b07492

Wan, W.-L., Lin, Y.-J., Shih, P.-C., Bow, Y.-R., Cui, Q., Chang, Y., Chia, W.-T., & Sung, H.-W. (2018). An in situ depot for continuous evolution of gaseous H_2 mediated by a magnesium passivation/activation cycle for treating osteoarthritis. *Angewandte Chemie International Edition*, *57*(31), 9875–9879. https://doi.org/10.1002/anie.201806159

Wan, W. L., Tian, B., Lin, Y. J., Korupalli, C., Lu, M. Y., Cui, Q., Wan, D., Chang, Y., & Sung, H. W. (2020). Photosynthesis-inspired H_2 generation using a chlorophyll-loaded liposomal nanoplatform to detect and scavenge excess ROS. *Nature Communications*, *11*(1), 534. https://doi.org/10.1038/s41467-020-14413-x

Wang, C.-C., Li, J.-R., Lv, X.-L., Zhang, Y.-Q., & Guo, G. (2014). Photocatalytic organic pollutants degradation in metal–organic frameworks. *Energy and Environmental Science*, *7*(9), 2831–2867. https://doi.org/10.1039/C4EE01299B

Wang, D., Viennois, E., Ji, K., Damera, K., Draganov, A., Zheng, Y., Dai, C., Merlin, D., & Wang, B. (2014). A click-and-release approach to CO prodrugs. *Chemical Communications (Cambridge, England)*, *50*(100), 15890–15893. https://doi.org/10.1039/c4cc07748b

Wang, H. Y., Wang, W. G., Si, G., Wang, F., Tung, C. H., & Wu, L. Z. (2010). Photocatalytic hydrogen evolution from rhenium(I) complexes to [FeFe] hydrogenase mimics in aqueous SDS micellar systems: A biomimetic pathway. *Langmuir*, *26*(12), 9766–9771. https://doi.org/10.1021/la101322s

Wang, Q., Ji, Y., Shi, J., & Wang, L. (2020). NIR-driven water splitting H_2 production nanoplatform for H_2-mediated cascade-amplifying synergetic cancer therapy. *ACS Applied Materials and Interfaces*, *12*(21), 23677–23688. https://doi.org/10.1021/acsami.0c03852

Wang, S.-B., Zhang, C., Ye, J.-J., Zou, M.-Z., Liu, C.-J., & Zhang, X.-Z. (2020). Near-infrared light responsive nanoreactor for simultaneous tumor photothermal therapy and carbon monoxide-mediated anti-inflammation. *ACS Central Science*, *6*(4), 555–565. https://doi.org/10.1021/acscentsci.9b01342

Wang, W., Ji, X., Du, Z., & Wang, B. (2017). Sulfur dioxide prodrugs: Triggered release of SO_2 via a click reaction. *Chemical Communications (Cambridge, England)*, *53*(8), 1370–1373. https://doi.org/10.1039/c6cc08844a

Wang, X. Y., Pu, J. H., Liu, Y., Ba, F., Cui, M. K., Li, K., Xie, Y., Nie, Y., Mi, Q. X., Li, T., Liu, L. L., Zhu, M. Z., & Zhong, C. (2019). Immobilization of functional nano-objects in living engineered bacterial biofilms for catalytic applications. *National Science Review*, *6*(5), 929–943. https://doi.org/10.1093/nsr/nwz104

Wang, Y., Huang, X., Tang, Y., Zou, J., Wang, P., Zhang, Y., Si, W., Huang, W., & Dong, X. (2018). A light-induced nitric oxide controllable release nano-platform based on diketopyrrolopyrrole derivatives for pH-responsive photodynamic/photothermal synergistic cancer therapy. *Chemical Science*, *9*(42), 8103–8109. https://doi.org/10.1039/c8sc03386b

Wang, Y., Yang, T., & He, Q. (2020). Strategies for engineering advanced nanomedicines for gas therapy of cancer. *National Science Review*, *7*(9), 1485–1512. https://doi.org/10.1093/nsr/nwaa034

Wang, Y., Zhang, J., Lv, X., Wang, L., Zhong, Z., Yang, D. P., Si, W., Zhang, T., & Dong, X. (2020). Mitoxantrone as photothermal agents for ultrasound/fluorescence imaging-guided chemo-phototherapy enhanced by intratumoral H_2O_2-induced CO. *Biomaterials*, *252*, 120111. https://doi.org/10.1016/j.biomaterials.2020.120111

Wang, Y. Q., Lv, P. X., Kong, L. S., Shen, W. B., & He, Q. J. (2021). Nanomaterial-mediated sustainable hydrogen supply induces lateral root formation via nitrate reductase-dependent nitric oxide. *Chemical Engineering Journal*, *405*, 126905. https://doi.org/10.1016/j.cej.2020.126905

Wang, Z., Zhang, Y., Ju, E., Liu, Z., Cao, F., Chen, Z., Ren, J., & Qu, X. (2018). Biomimetic nanoflowers by self-assembly of nanozymes to induce intracellular oxidative damage against hypoxic tumors. *Nature Communications*, *9*(1), 3334. https://doi.org/10.1038/s41467-018-05798-x

Wecksler, S. R., Mikhailovsky, A., Korystov, D., & Ford, P. C. (2006). A two-photon antenna for photochemical delivery of nitric oxide from a water-soluble, dye-derivatized iron nitrosyl complex using NIR light. *Journal of the American Chemical Society*, *128*(11), 3831–3837. https://doi.org/10.1021/ja057977u

Wheatley, P. S., Butler, A. R., Crane, M. S., Fox, S., Xiao, B., Rossi, A. G., Megson, I. L., & Morris, R. E. (2006). NO-releasing zeolites and their antithrombotic properties. *Journal of the American Chemical Society*, *128*(2), 502–509. https://doi.org/10.1021/ja0503579

Wu, C., Wang, D., Cen, M., Cao, L., Ding, Y., Wang, J., Yuan, X., Wang, Y., Chen, T., & Yao, Y. (2020). Mitochondria-targeting NO gas nanogenerator for augmenting mild photothermal therapy in the NIR-II biowindow. *Chemical Communications (Cambridge, England)*, *56*(92), 14491–14494. https://doi.org/10.1039/d0cc05125j

Wu, D., Duan, X. H., Guan, Q. Q., Liu, J., Yang, X., Zhang, F., Huang, P., Shen, J., Shuai, X. T., & Cao, Z. (2019). Mesoporous polydopamine carrying manganese carbonyl responds to tumor microenvironment for multimodal imaging-guided cancer therapy. *Advanced Functional Materials*, *29*(16), 1900095. https://doi.org/10.1002/adfm.201900095

Wu, L., & Wang, R. (2005). Carbon monoxide: Endogenous production, physiological functions, and pharmacological applications. *Pharmacological Reviews*, *57*(4), 585–630. https://doi.org/10.1124/pr.57.4.3

Wu, X. J., Tang, X. P., Xian, M., & Wang, P. G. (2001). Glycosylated diazeniumdiolates: A novel class of enzyme-activated nitric oxide donors. *Tetrahedron Letters*, *42*(23), 3779–3782. https://doi.org/10.1016/S0040-4039(01)00614-1

Wu, Y., Su, L., Yuan, M., Chen, T., Ye, J., Jiang, Y., Song, J., & Yang, H. (2021). In vivo X-ray triggered catalysis of H_2 generation for Cancer synergistic gas radiotherapy. *Angewandte Chemie International Edition*, *60*(23), 12868–12875.

Wu, Y., Yuan, M., Song, J., Chen, X., & Yang, H. (2019). Hydrogen gas from inflammation treatment to cancer therapy. *ACS Nano*, *13*(8), 8505–8511. https://doi.org/10.1021/acsnano.9b05124

Xie, C., Cen, D., Ren, Z., Wang, Y., Wu, Y., Li, X., Han, G., & Cai, X. (2020). FeS@BSA nanoclusters to enable H_2S-amplified ROS-based therapy with MRI guidance. *Advanced Science*, *7*(7), 1903512. https://doi.org/10.1002/advs.201903512

Xie, Z., Liang, S., Cai, X., Ding, B., Huang, S., Hou, Z., Ma, P. A., Cheng, Z., & Lin, J. (2019). O_2-Cu/ZIF-8@Ce6/ZIF-8@F127 composite as a tumor microenvironment-responsive nanoplatform with enhanced photo-/chemodynamic antitumor efficacy. *ACS Applied Materials and Interfaces*, *11*(35), 31671–31680. https://doi.org/10.1021/acsami.9b10685

Xu, M., Lu, Q., Song, Y., Yang, L., Li, J., & Li, N. (2020). Enhanced Bax upregulating in mitochondria for deep tumor therapy based on SO_2 prodrug loaded Au–Ag hollow nanotriangles. *Biomaterials*, *250*, 120076. https://doi.org/10.1016/j.biomaterials.2020.120076

Xu, S., Yang, C. T., Meng, F. H., Pacheco, A., Chen, L., & Xian, M. (2016). Ammonium tetrathiomolybdate as a water-soluble and slow-release hydrogen sulfide donor. *Bioorganic and Medicinal Chemistry Letters*, *26*(6), 1585–1588. https://doi.org/10.1016/j.bmcl.2016.02.005

Yamamoto, R., Homma, K., Suzuki, S., Sano, M., & Sasaki, J. (2019). Hydrogen gas distribution in organs after inhalation: Real-time monitoring of tissue hydrogen concentration in rat. *Scientific Reports*, *9*(1), 1255. https://doi.org/10.1038/s41598-018-38180-4

Yang, B., Chen, Y., & Shi, J. (2019). Nanocatalytic medicine. *Advanced Materials*, *31*(39), 1901778. https://doi.org/10.1002/adma.201901778

Yang, L., Wen, Z., Long, Y., Huang, N., Cheng, Y., Zhao, L., & Zheng, H. (2016). A H(+)-triggered bubble-generating nanosystem for killing cancer cells. *Chemical Communications (Cambridge, England)*, *52*(72), 10838–10841. https://doi.org/10.1039/c6cc04511a

Yang, T., Jin, Z., Wang, Z., Zhao, P., Zhao, B., Fan, M., Chen, L., Wang, T., Su, B.-L., & He, Q. (2018). Intratumoral high-payload delivery and acid-responsive release of H_2 for efficient cancer therapy using the ammonia borane-loaded mesoporous silica nanomedicine. *Applied Materials Today*, *11*, 136–143. https://doi.org/10.1016/j.apmt.2018.01.008

Yao, J., Liu, Y., Wang, J., Jiang, Q., She, D., Guo, H., Sun, N., Pang, Z., Deng, C., Yang, W., & Shen, S. (2019). On-demand CO release for amplification of chemotherapy by MOF functionalized magnetic carbon nanoparticles with NIR irradiation. *Biomaterials*, *195*, 51–62. https://doi.org/10.1016/j.biomaterials.2018.12.029

Yao, X., Yang, P., Jin, Z., Jiang, Q., Guo, R., Xie, R., He, Q., & Yang, W. (2019). Multifunctional nanoplatform for photoacoustic imaging-guided combined therapy enhanced by CO induced ferroptosis. *Biomaterials*, *197*, 268–283. https://doi.org/10.1016/j.biomaterials.2019.01.026

Zhang, B., Wang, F., Zhou, H., Gao, D., Yuan, Z., Wu, C., & Zhang, X. (2019). Polymer dots compartmentalized in liposomes as a photocatalyst for in situ hydrogen therapy. *Angewandte Chemie International Edition*, *58*(9), 2744–2748. https://doi.org/10.1002/anie.201813066

Zhang, C., Zheng, D. W., Li, C. X., Zou, M. Z., Yu, W. Y., Liu, M. D., Peng, S. Y., Zhong, Z. L., & Zhang, X. Z. (2019). Hydrogen gas improves photothermal therapy of tumor and restrains the relapse of distant dormant tumor. *Biomaterials*, *223*, 119472. https://doi.org/10.1016/j.biomaterials.2019.119472

Zhang, K., Xu, H., Chen, H., Jia, X., Zheng, S., Cai, X., Wang, R., Mou, J., Zheng, Y., & Shi, J. (2015). CO_2 bubbling-based 'nanobomb' system for targetedly suppressing Panc-1 pancreatic tumor via low intensity ultrasound-activated inertial cavitation. *Theranostics*, *5*(11), 1291–1302.

Zhang, P., Li, Y., Tang, Y., Shen, H., Li, J., Yi, Z., Ke, Q., & Xu, H. (2020). Copper-based metal–organic framework as a controllable nitric oxide-releasing vehicle for enhanced diabetic wound healing. *ACS Applied Materials and Interfaces*, *12*(16), 18319–18331. https://doi.org/10.1021/acsami.0c01792

Zhang, X., Du, J., Guo, Z., Yu, J., Gao, Q., Yin, W., Zhu, S., Gu, Z., & Zhao, Y. (2019). Efficient near infrared light triggered nitric oxide release nanocomposites for sensitizing mild photothermal therapy. *Advanced Science*, *6*(3), 1801122. https://doi.org/10.1002/advs.201801122

Zhang, X., Guo, Z., Liu, J., Tian, G., Chen, K., Yu, S., & Gu, Z. (2017). Near infrared light triggered nitric oxide releasing platform based on upconversion nanoparticles for synergistic therapy of cancer stem-like cells. *Science Bulletin*, *62*(14), 985–996. https://doi.org/10.1016/j.scib.2017.06.010

Zhang, X., Tian, G., Yin, W., Wang, L., Zheng, X., Yan, L., Li, J., Su, H., Chen, C., Gu, Z., & Zhao, Y. (2015). Controllable generation of nitric oxide by near-infrared-sensitized upconversion nanoparticles for tumor therapy. *Advanced Functional Materials*, *25*(20), 3049–3056. https://doi.org/10.1002/adfm.201404402

Zhang, Y., Bo, S., Feng, T., Qin, X., Wan, Y., Jiang, S., Li, C., Lin, J., Wang, T., Zhou, X., Jiang, Z. X., & Huang, P. (2019). A versatile theranostic nanoemulsion for architecture-dependent multimodal imaging and dually augmented photodynamic therapy. *Advanced Materials*, *31*(21), e1806444. https://doi.org/10.1002/adma.201806444

Zhang, Y., Guan, Y., Ge, S., Yuan, A., Wu, J., & Hu, Y. (2017). Light-responsive CO_2 bubble-generating polymeric micelles for tumor cell ablation. *MedChemComm*, *8*(2), 405–407. https://doi.org/10.1039/c6md00625f

Zhang, Y., Shen, W., Zhang, P., Chen, L., & Xiao, C. (2020). GSH-triggered release of sulfur dioxide gas to regulate redox balance for enhanced photodynamic therapy. *Chemical Communications (Cambridge, England)*, *56*(42), 5645–5648. https://doi.org/10.1039/d0cc00470g

Zhang, Y. H., Liu, H. F., Dai, X. Y., Li, H., Zhou, X. H., Chen, S. Z., Zhang, J. C., Liang, X. J., & Li, Z. H. (2021). *Cyanobacteria*-based near-infrared light-excited self-supplying oxygen system for enhanced photodynamic therapy of hypoxic tumors. *Nano Research*, *14*(3), 667–673. https://doi.org/10.1007/s12274-020-3094-0

Zhao, B., Wang, Y., Yao, X., Chen, D., Fan, M., Jin, Z., & He, Q. (2021). Photocatalysis-mediated drug-free sustainable cancer therapy using nanocatalyst. *Nature Communications*, *12*(1), 1345. https://doi.org/10.1038/s41467-021-21618-1

Zhao, B., Zhao, P., Jin, Z., Fan, M., Meng, J., & He, Q. (2019). Programmed ROS/CO-releasing nanomedicine for synergetic chemodynamic-gas therapy of cancer. *Journal of Nanobiotechnology*, *17*(1), 75. https://doi.org/10.1186/s12951-019-0507-x

Zhao, P., Jin, Z., Chen, Q., Yang, T., Chen, D., Meng, J., Lu, X., Gu, Z., & He, Q. (2018). Local generation of hydrogen for enhanced photothermal therapy. *Nature Communications*, *9*(1), 4241. https://doi.org/10.1038/s41467-018-06630-2

Zhao, Y., Bhushan, S., Yang, C., Otsuka, H., Stein, J. D., Pacheco, A., Peng, B., Devarie-Baez, N. O., Aguilar, H. C., Lefer, D. J., & Xian, M. (2013). Controllable hydrogen sulfide donors and their activity against myocardial ischemia–reperfusion injury. *ACS Chemical Biology*, *8*(6), 1283–1290. https://doi.org/10.1021/cb400090d

Zhao, Y., Kang, J., Park, C. M., Bagdon, P. E., Peng, B., & Xian, M. (2014). Thiol-activated gem-dithiols: A new class of controllable hydrogen sulfide donors. *Organic Letters*, *16*(17), 4536–4539. https://doi.org/10.1021/ol502088m

Zhao, Y., Yang, C., Organ, C., Li, Z., Bhushan, S., Otsuka, H., Pacheco, A., Kang, J., Aguilar, H. C., Lefer, D. J., & Xian, M. (2015). Design, synthesis, and cardioprotective effects of N-mercapto-based hydrogen sulfide donors. *Journal of Medicinal Chemistry*, *58*(18), 7501–7511. https://doi.org/10.1021/acs.jmedchem.5b01033

Zheng, D.-W., Chen, Y., Li, Z.-H., Xu, L., Li, C.-X., Li, B., Fan, J.-X., Cheng, S.-X., & Zhang, X.-Z. (2018). Optically-controlled bacterial metabolite for cancer therapy. *Nature Communications*, *9*(1), 1680. https://doi.org/10.1038/s41467-018-03233-9

Zheng, D. W., Li, B., Li, C. X., Xu, L., Fan, J. X., Lei, Q., & Zhang, X. Z. (2017). Photocatalyzing CO_2 to CO for enhanced cancer therapy. *Advanced Materials*, *29*(44), 1703822. https://doi.org/10.1002/adma.201703822

Zheng, Y., Ji, X., Yu, B., Ji, K., Gallo, D., Csizmadia, E., Zhu, M., Choudhury, M. R., De La Cruz, L. K. C., Chittavong, V., Pan, Z., Yuan, Z., Otterbein, L. E., & Wang, B. (2018). Enrichment-triggered prodrug activation demonstrated through mitochondria-targeted delivery of doxorubicin and carbon monoxide. *Nature Chemistry*, *10*(7), 787–794. https://doi.org/10.1038/s41557-018-0055-2

Zheng, Z., Chen, Q., Dai, R., Jia, Z., Yang, C., Peng, X., & Zhang, R. (2020). A continuous stimuli-responsive system for NIR-II fluorescence/photoacoustic imaging guided photothermal/gas synergistic therapy. *Nanoscale*, *12*(21), 11562–11572. https://doi.org/10.1039/d0nr02543g

Zhou, G. X., Wang, Y. S., Jin, Z. K., Zhao, P. H., Zhang, H., Wen, Y. Y., & He, Q. J. (2019). Porphyrin-palladium hydride MOF nanoparticles for tumor-targeting photoacoustic imaging-guided hydrogenothermal cancer therapy. *Nanoscale Horizons*, *4*(5), 1185–1193. https://doi.org/10.1039/c9nh00021f

Zobi, F., Quaroni, L., Santoro, G., Zlateva, T., Blacque, O., Sarafimov, B., Schaub, M. C., & Bogdanova, A. Y. (2013). Live-fibroblast IR imaging of a cytoprotective PhotoCORM activated with visible light. *Journal of Medicinal Chemistry*, *56*(17), 6719–6731. https://doi.org/10.1021/jm400527k

How to cite this article: Gong, W., Xia, C., & He, Q. (2022). Therapeutic gas delivery strategies. *Wiley Interdisciplinary Reviews: Nanomedicine and Nanobiotechnology*, *14*(1), e1744. https://doi.org/10.1002/wnan.1744